UNITED STATES AIR FORCE

SUMMER RESEARCH PROGRAM -- 1998

GRADUATE STUDENT RESEARCH PROGRAM FINAL REPORTS

VOLUME 11

ARNOLD ENGINEERING DEVELOPMENT CENTER

WILFORD HALL MEDCIAL CENTER

RESEARCH & DEVELOPMENT LABORATORIES

5800 Uplander Way

Culver City, CA 90230-6608

Program Director, RDL
Gary Moore

Program Manager, AFOSR
Colonel Jan Cerveny

Program Manager, RDL
Scott Licoscos

Program Administrator, RDL
Johnetta Thompson

Program Administrator, RDL
Rebecca Kelly-Clemmons

Submitted to:

AIR FORCE OFFICE OF SCIENTIFIC RESEARCH

Bolling Air Force Base

Washington, D.C.

December 1998

PREFACE

Reports in this volume are numbered consecutively beginning with number 1. Each report is paginated with the report number followed by consecutive page numbers, e.g., 1-1, 1-2, 1-3; 2-1, 2-2, 2-3.

This document is one of a set of 15 volumes describing the 1998 AFOSR Summer Research Program. The following volumes comprise the set:

VOLUME	TITLE
1	Program Management Report
	Summer Faculty Research Program (SFRP) Reports
2	Armstrong Laboratory
3	Phillips Laboratory
4	Rome Laboratory
5A & 5B	Wright Laboratory
6	Arnold Engineering Development Center, Air Logistics Centers, United States Air Force Academy and Wilford Hall Medical Center
	Graduate Student Research Program (GSRP) Reports
7	Armstrong Laboratory
8	Phillips Laboratory
9	Rome Laboratory
10	Wright Laboratory
11	Arnold Engineering Development Center, and Wilford Hall Medical Center
	High School Apprenticeship Program (HSAP) Reports
12	Armstrong Laboratory
13	Phillips Laboratory
14	Rome Laboratory
15A, 15B & 15C	Wright Laboratory

REPORT DOCUMENTATION PAGE

AFRL-SR-BL-TR-00-

0787

reviewing
information

1. AGENCY USE ONLY *(Leave blank)*	2. REPORT DATE	3. REPORT TYPE AND DATES COVERED
	December, 1998	

4. TITLE AND SUBTITLE
1998 Summer Research Program (SRP), Graduate Student Research Program (GSRP), Final Reports, Volume 11, Arnold Eng. Development Center and Wilford Hall Medical Center

5. FUNDING NUMBERS
F49620-93-C-0063

6. AUTHOR(S)
Gary Moore

7. PERFORMING ORGANIZATION NAME(S) AND ADDRESS(ES)
Research & Development Laboratories (RDL)
5800 Uplander Way
Culver City, CA 90230-6608

8. PERFORMING ORGANIZATION REPORT NUMBER

9. SPONSORING/MONITORING AGENCY NAME(S) AND ADDRESS(ES)
Air Force Office of Scientific Research (AFOSR)
801 N. Randolph St.
Arlington, VA 22203-1977

10. SPONSORING/MONITORING AGENCY REPORT NUMBER

11. SUPPLEMENTARY NOTES

12a. DISTRIBUTION AVAILABILITY STATEMENT
Approved for Public Release

12b. DISTRIBUTION CODE

13. ABSTRACT *(Maximum 200 words)*

The United States Air Force Summer Research Program (USAF-SRP) is designed to introduce university, college, and technical institute faculty members, graduate students, and high school students to Air Force research. This is accomplished by the faculty members (Summer Faculty Research Program, (SFRP)), graduate students (Graduate Student Research Program (GSRP)), and high school students (High School Apprenticeship Program (HSAP)) being selected on a nationally advertised competitive basis during the summer intersession period to perform research at Air Force Research Laboratory (AFRL) Technical Directorates, Air Force Air Logistics Centers (ALC), and other AF Laboratories. This volume consists of a program overview, program management statistics, and the final technical reports from the GSRP participants at the Arnold Engineering Development Center and Wilford Hall Medical Center.

14. SUBJECT TERMS
Air Force Research, Air Force, Engineering, Laboratories, Reports, Summer, Universities, Faculty, Graduate Student, High School Student

15. NUMBER OF PAGES

16. PRICE CODE

17. SECURITY CLASSIFICATION OF REPORT	18. SECURITY CLASSIFICATION OF THIS PAGE	19. SECURITY CLASSIFICATION OF ABSTRACT	20. LIMITATION OF ABSTRACT
Unclassified	Unclassified	Unclassified	UL

GENERAL INSTRUCTIONS FOR COMPLETING SF 298

The Report Documentation Page (RDP) is used in announcing and cataloging reports. It is important that this information be consistent with the rest of the report, particularly the cover and title page. Instructions for filling in each block of the form follow. It is important to ***stay within the lines*** to meet ***optical scanning requirements.***

Block 1. Agency Use Only *(Leave blank)*.

Block 2. Report Date. Full publication date including day, month, and year, if available (e.g. 1 Jan 88). Must cite at least the year.

Block 3. Type of Report and Dates Covered. State whether report is interim, final, etc. If applicable, enter inclusive report dates (e.g. 10 Jun 87 - 30 Jun 88).

Block 4. Title and Subtitle. A title is taken from the part of the report that provides the most meaningful and complete information. When a report is prepared in more than one volume, repeat the primary title, add volume number, and include subtitle for the specific volume. On classified documents enter the title classification in parentheses.

Block 5. Funding Numbers. To include contract and grant numbers; may include program element number(s), project number(s), task number(s), and work unit number(s). Use the following labels:

C - Contract	**PR** - Project
G - Grant	**TA** - Task
PE - Program Element	**WU** - Work Unit Accession No.

Block 6. Author(s). Name(s) of person(s) responsible for writing the report, performing the research, or credited with the content of the report. If editor or compiler, this should follow the name(s).

Block 7. Performing Organization Name(s) and Address(es). Self-explanatory.

Block 8. Performing Organization Report Number. Enter the unique alphanumeric report number(s) assigned by the organization performing the report.

Block 9. Sponsoring/Monitoring Agency Name(s) and Address(es). Self-explanatory.

Block 10. Sponsoring/Monitoring Agency Report Number. *(If known)*

Block 11. Supplementary Notes. Enter information not included elsewhere such as: Prepared in cooperation with....; Trans. of....; To be published in.... When a report is revised, include a statement whether the new report supersedes or supplements the older report.

Block 12a. Distribution/Availability Statement. Denotes public availability or limitations. Cite any availability to the public. Enter additional limitations or special markings in all capitals (e.g. NOFORN, REL, ITAR).

DOD -	See DoDD 5230.24, "Distribution Statements on Technical Documents."
DOE -	See authorities.
NASA -	See Handbook NHB 2200.2.
NTIS -	Leave blank.

Block 12b. Distribution Code.

DOD -	Leave blank.
DOE -	Enter DOE distribution categories from the Standard Distribution for Unclassified Scientific and Technical Reports.
	Leave blank.
NASA -	Leave blank.
NTIS -	

Block 13. Abstract. Include a brief *(Maximum 200 words)* factual summary of the most significant information contained in the report.

Block 14. Subject Terms. Keywords or phrases identifying major subjects in the report.

Block 15. Number of Pages. Enter the total number of pages.

Block 16. Price Code. Enter appropriate price code *(NTIS only)*.

Blocks 17. - 19. Security Classifications. Self- explanatory. Enter U.S. Security Classification in accordance with U.S. Security Regulations (i.e., UNCLASSIFIED). If form contains classified information, stamp classification on the top and bottom of the page.

Block 20. Limitation of Abstract. This block must be completed to assign a limitation to the abstract. Enter either UL (unlimited) or SAR (same as report). An entry in this block is necessary if the abstract is to be limited. If blank, the abstract is assumed to be unlimited.

SRP Final Report Table of Contents

SRP Final Report Table of Contents

SRP Final Report Table of Contents

SRP Final Report Table of Contents

SRP Final Report Table of Contents

SRP Final Report Table of Contents

1. INTRODUCTION

The Summer Research Program (SRP), sponsored by the Air Force Office of Scientific Research (AFOSR), offers paid opportunities for university faculty, graduate students, and high school students to conduct research in U.S. Air Force research laboratories nationwide during the summer.

Introduced by AFOSR in 1978, this innovative program is based on the concept of teaming academic researchers with Air Force scientists in the same disciplines using laboratory facilities and equipment not often available at associates' institutions.

The Summer Faculty Research Program (SFRP) is open annually to approximately 150 faculty members with at least two years of teaching and/or research experience in accredited U.S. colleges, universities, or technical institutions. SFRP associates must be either U.S. citizens or permanent residents.

The Graduate Student Research Program (GSRP) is open annually to approximately 100 graduate students holding a bachelor's or a master's degree; GSRP associates must be U.S. citizens enrolled full time at an accredited institution.

The High School Apprentice Program (HSAP) annually selects about 125 high school students located within a twenty mile commuting distance of participating Air Force laboratories.

AFOSR also offers its research associates an opportunity, under the Summer Research Extension Program (SREP), to continue their AFOSR-sponsored research at their home institutions through the award of research grants. In 1994 the maximum amount of each grant was increased from $20,000 to $25,000, and the number of AFOSR-sponsored grants decreased from 75 to 60. A separate annual report is compiled on the SREP.

The numbers of projected summer research participants in each of the three categories and SREP "grants" are usually increased through direct sponsorship by participating laboratories.

AFOSR's SRP has well served its objectives of building critical links between Air Force research laboratories and the academic community, opening avenues of communications and forging new research relationships between Air Force and academic technical experts in areas of national interest, and strengthening the nation's efforts to sustain careers in science and engineering. The success of the SRP can be gauged from its growth from inception (see Table 1) and from the favorable responses the 1997 participants expressed in end-of-tour SRP evaluations (Appendix B).

AFOSR contracts for administration of the SRP by civilian contractors. The contract was first awarded to Research & Development Laboratories (RDL) in September 1990. After completion of the 1990 contract, RDL (in 1993) won the recompetition for the basic year and four 1-year options.

2. PARTICIPATION IN THE SUMMER RESEARCH PROGRAM

The SRP began with faculty associates in 1979; graduate students were added in 1982 and high school students in 1986. The following table shows the number of associates in the program each year.

YEAR	SRP Participation, by Year			TOTAL
	SFRP	GSRP	HSAP	
1979	70			70
1980	87			87
1981	87			87
1982	91	17		108
1983	101	53		154
1984	152	84		236
1985	154	92		246
1986	158	100	42	300
1987	159	101	73	333
1988	153	107	101	361
1989	168	102	103	373
1990	165	121	132	418
1991	170	142	132	444
1992	185	121	159	464
1993	187	117	136	440
1994	192	117	133	442
1995	190	115	137	442
1996	188	109	138	435
1997	148	98	140	427
1998	85	40	88	213

Beginning in 1993, due to budget cuts, some of the laboratories weren't able to afford to fund as many associates as in previous years. Since then, the number of funded positions has remained fairly constant at a slightly lower level.

3. RECRUITING AND SELECTION

The SRP is conducted on a nationally advertised and competitive-selection basis. The advertising for faculty and graduate students consisted primarily of the mailing of 8,000 52-page SRP brochures to chairpersons of departments relevant to AFOSR research and to administrators of grants in accredited universities, colleges, and technical institutions. Historically Black Colleges and Universities (HBCUs) and Minority Institutions (MIs) were included. Brochures also went to all participating USAF laboratories, the previous year's participants, and numerous individual requesters (over 1000 annually).

RDL placed advertisements in the following publications: *Black Issues in Higher Education, Winds of Change,* and *IEEE Spectrum.* Because no participants list either *Physics Today* or *Chemical & Engineering News* as being their source of learning about the program for the past several years, advertisements in these magazines were dropped, and the funds were used to cover increases in brochure printing costs.

High school applicants can participate only in laboratories located no more than 20 miles from their residence. Tailored brochures on the HSAP were sent to the head counselors of 180 high schools in the vicinity of participating laboratories, with instructions for publicizing the program in their schools. High school students selected to serve at Wright Laboratory's Armament Directorate (Eglin Air Force Base, Florida) serve eleven weeks as opposed to the eight weeks normally worked by high school students at all other participating laboratories.

Each SFRP or GSRP applicant is given a first, second, and third choice of laboratory. High school students who have more than one laboratory or directorate near their homes are also given first, second, and third choices.

Laboratories make their selections and prioritize their nominees. AFOSR then determines the number to be funded at each laboratory and approves laboratories' selections.

Subsequently, laboratories use their own funds to sponsor additional candidates. Some selectees do not accept the appointment, so alternate candidates are chosen. This multi-step selection procedure results in some candidates being notified of their acceptance after scheduled deadlines. The total applicants and participants for 1998 are shown in this table.

1998 Applicants and Participants			
PARTICIPANT CATEGORY	TOTAL APPLICANTS	SELECTEES	DECLINING SELECTEES
SFRP	382	85	13
(HBCU/MI)	(0)	(0)	(0)
GSRP	130	40	7
(HBCU/MI)	(0)	(0)	(0)
HSAP	328	88	22
TOTAL	840	213	42

4. SITE VISITS

During June and July of 1998, representatives of both AFOSR/NI and RDL visited each participating laboratory to provide briefings, answer questions, and resolve problems for both laboratory personnel and participants. The objective was to ensure that the SRP would be as constructive as possible for all participants. Both SRP participants and RDL representatives found these visits beneficial. At many of the laboratories, this was the only opportunity for all participants to meet at one time to share their experiences and exchange ideas.

5. HISTORICALLY BLACK COLLEGES AND UNIVERSITIES AND MINORITY INSTITUTIONS (HBCU/MIs)

Before 1993, an RDL program representative visited from seven to ten different HBCU/MIs annually to promote interest in the SRP among the faculty and graduate students. These efforts were marginally effective, yielding a doubling of HBCI/MI applicants. In an effort to achieve AFOSR's goal of 10% of all applicants and selectees being HBCU/MI qualified, the RDL team decided to try other avenues of approach to increase the number of qualified applicants. Through the combined efforts of the AFOSR Program Office at Bolling AFB and RDL, two very active minority groups were found, HACU (Hispanic American Colleges and Universities) and AISES (American Indian Science and Engineering Society). RDL is in communication with representatives of each of these organizations on a monthly basis to keep up with the their activities and special events. Both organizations have widely-distributed magazines/quarterlies in which RDL placed ads.

Since 1994 the number of both SFRP and GSRP HBCU/MI applicants and participants has increased ten-fold, from about two dozen SFRP applicants and a half dozen selectees to over 100 applicants and two dozen selectees, and a half-dozen GSRP applicants and two or three selectees to 18 applicants and 7 or 8 selectees. Since 1993, the SFRP had a two-fold applicant increase and a two-fold selectee increase. Since 1993, the GSRP had a three-fold applicant increase and a three to four-fold increase in selectees.

In addition to RDL's special recruiting efforts, AFOSR attempts each year to obtain additional funding or use leftover funding from cancellations the past year to fund HBCU/MI associates.

SRP HBCU/MI Participation, By Year				
YEAR	SFRP		GSRP	
	Applicants	Participants	Applicants	Participants
1985	76	23	15	11
1986	70	18	20	10
1987	82	32	32	10
1988	53	17	23	14
1989	39	15	13	4
1990	43	14	17	3
1991	42	13	8	5
1992	70	13	9	5
1993	60	13	6	2
1994	90	16	11	6
1995	90	21	20	8
1996	119	27	18	7

6. SRP FUNDING SOURCES

Funding sources for the 1998 SRP were the AFOSR-provided slots for the basic contract and laboratory funds. Funding sources by category for the 1998 SRP selected participants are shown here.

1998 SRP FUNDING CATEGORY	SFRP	GSRP	HSAP
AFOSR Basic Allocation Funds	67	38	75
USAF Laboratory Funds	17	2	13
Slots Added by AFOSR (Leftover Funds)	0	0	0
HBCU/MI By AFOSR (Using Procured Addn'l Funds)	0	0	N/A
TOTAL	84	40	88

7. COMPENSATION FOR PARTICIPANTS

Compensation for SRP participants, per five-day work week, is shown in this table.

1998 SRP Associate Compensation

PARTICIPANT CATEGORY	1991	1992	1993	1994	1995	1996	1997	1998
Faculty Members	$690	$718	$740	$740	$740	$770	$770	$793
Graduate Student (Master's Degree)	$425	$442	$455	$455	$455	$470	$470	$484
Graduate Student (Bachelor's Degree)	$365	$380	$391	$391	$391	$400	$400	$412
High School Student (First Year)	$200	$200	$200	$200	$200	$200	$200	$200
High School Student (Subsequent Years)	$240	$240	$240	$240	$240	$240	$240	$240

The program also offered associates whose homes were more than 50 miles from the laboratory an expense allowance (seven days per week) of $52/day for faculty and $41/day for graduate students. Transportation to the laboratory at the beginning of their tour and back to their home destinations at the end was also reimbursed for these participants. Of the combined SFRP and GSRP associates, 65 % claimed travel reimbursements at an average round-trip cost of $730.

Faculty members were encouraged to visit their laboratories before their summer tour began. All costs of these orientation visits were reimbursed. Forty-three percent (85 out of 188) of faculty associates took orientation trips at an average cost of $449. By contrast, in 1993, 58 % of SFRP associates elected to take an orientation visits at an average cost of $685; that was the highest

percentage of associates opting to take an orientation trip since RDL has administered the SRP, and the highest average cost of an orientation trip.

Program participants submitted biweekly vouchers countersigned by their laboratory research focal point, and RDL issued paychecks so as to arrive in associates' hands two weeks later.

This is the third year of using direct deposit for the SFRP and GSRP associates. The process went much more smoothly with respect to obtaining required information from the associates, about 15% of the associates' information needed clarification in order for direct deposit to properly function as opposed to 7% from last year. The remaining associates received their stipend and expense payments via checks sent in the US mail.

HSAP program participants were considered actual RDL employees, and their respective state and federal income tax and Social Security were withheld from their paychecks. By the nature of their independent research, SFRP and GSRP program participants were considered to be consultants or independent contractors. As such, SFRP and GSRP associates were responsible for their own income taxes, Social Security, and insurance.

8. CONTENTS OF THE 1998 REPORT

The complete set of reports for the 1998 SRP includes this program management report (Volume 1) augmented by fifteen volumes of final research reports by the 1998 associates, as indicated below:

1998 SRP Final Report Volume Assignments

LABORATORY	SFRP	GSRP	HSAP
Armstrong	2	7	12
Phillips	3	8	13
Rome	4	9	14
Wright	5A, 5B	10	15
AEDC, ALCs, USAFA, WHMC	6	11	

APPENDIX A -- PROGRAM STATISTICAL SUMMARY

A. Colleges/Universities Represented

Selected SFRP associates represented 169 different colleges, universities, and institutions, GSRP associates represented 95 different colleges, universities, and institutions.

B. States Represented

SFRP -Applicants came from 47 states plus Washington D.C. Selectees represent 44 states.

GSRP - Applicants came from 44 states. Selectees represent 32 states.

HSAP - Applicants came from thirteen states. Selectees represent nine states.

Total Number of Participants	
SFRP	85
GSRP	40
HSAP	88
TOTAL	213

Degrees Represented			
	SFRP	GSRP	TOTAL
Doctoral	83	0	83
Master's	1	3	4
Bachelor's	0	22	22
TOTAL	186	25	109

SFRP Academic Titles	
Assistant Professor	36
Associate Professor	34
Professor	15
Instructor	0
Chairman	0
Visiting Professor	0
Visiting Assoc. Prof.	0
Research Associate	0
TOTAL	85

Source of Learning About the SRP		
Category	Applicants	Selectees
Applied/participated in prior years	177	47
Colleague familiar with SRP	104	24
Brochure mailed to institution	101	21
Contact with Air Force laboratory	101	39
IEEE Spectrum	12	1
BIIHE	4	0
Other source	117	30
TOTAL	616	162

APPENDIX B -- SRP EVALUATION RESPONSES

1. OVERVIEW

Evaluations were completed and returned to RDL by four groups at the completion of the SRP. The number of respondents in each group is shown below.

Table B-1. Total SRP Evaluations Received

Evaluation Group	Responses
SFRP & GSRPs	100
HSAPs	75
USAF Laboratory Focal Points	84
USAF Laboratory HSAP Mentors	6

All groups indicate unanimous enthusiasm for the SRP experience.

The summarized recommendations for program improvement from both associates and laboratory personnel are listed below:

A. Better preparation on the labs' part prior to associates' arrival (i.e., office space, computer assets, clearly defined scope of work).

B. Faculty Associates suggest higher stipends for SFRP associates.

C. Both HSAP Air Force laboratory mentors and associates would like the summer tour extended from the current 8 weeks to either 10 or 11 weeks; the groups state it takes 4-6 weeks just to get high school students up-to-speed on what's going on at laboratory. (Note: this same argument was used to raise the faculty and graduate student participation time a few years ago.)

2. 1998 USAF LABORATORY FOCAL POINT (LFP) EVALUATION RESPONSES

The summarized results listed below are from the 84 LFP evaluations received.

1. LFP evaluations received and associate preferences:

Table B-2. Air Force LFP Evaluation Responses (By Type)

		How Many Associates Would You Prefer To Get ? (% Response)											
		SFRP				GSRP (w/Univ Professor)				GSRP (w/o Univ Professor)			
Lab	Evals Recv'd	0	1	2	3+	0	1	2	3+	0	1	2	3+
AEDC	0	-	-	-	-	-	-	-	-	-	-	-	-
WHMC	0	-	-	-	-	-	-	-	-	-	-	-	-
AL	7	28	28	28	14	54	14	28	0	86	0	14	0
USAFA	1	0	100	0	0	100	0	0	0	0	100	0	0
PL	25	40	40	16	4	88	12	0	0	84	12	4	0
RL	5	60	40	0	0	80	10	0	0	100	0	0	0
WL	46	30	43	20	6	78	17	4	0	93	4	2	0
Total	**84**	**32%**	**50%**	**13%**	**5%**	**80%**	**11%**	**6%**	**0%**	**73%**	**23%**	**4%**	**0%**

LFP Evaluation Summary. The summarized responses, by laboratory, are listed on the following page. LFPs were asked to rate the following questions on a scale from 1 (below average) to 5 (above average).

2. LFPs involved in SRP associate application evaluation process:
   a. Time available for evaluation of applications:
   b. Adequacy of applications for selection process:
3. Value of orientation trips:
4. Length of research tour:
5. a. Benefits of associate's work to laboratory:
   b. Benefits of associate's work to Air Force:
6. a. Enhancement of research qualifications for LFP and staff:
   b. Enhancement of research qualifications for SFRP associate:
   c. Enhancement of research qualifications for GSRP associate:
7. a. Enhancement of knowledge for LFP and staff:
   b. Enhancement of knowledge for SFRP associate:
   c. Enhancement of knowledge for GSRP associate:
8. Value of Air Force and university links:
9. Potential for future collaboration:
10. a. Your working relationship with SFRP:
    b. Your working relationship with GSRP:
11. Expenditure of your time worthwhile:

(Continued on next page)

12. Quality of program literature for associate:
13. a. Quality of RDL's communications with you:
    b. Quality of RDL's communications with associates:
14. Overall assessment of SRP:

Table B-3. Laboratory Focal Point Reponses to above questions

	AEDC	*AL*	*USAFA*	*PL*	*RL*	*WHMC*	*WL*
# Evals Recv'd	0	7	1	14	5	0	46
Question #							
2	-	86 %	0 %	88 %	80 %	-	85 %
2a	-	4.3	n/a	3.8	4.0	-	3.6
2b	-	4.0	n/a	3.9	4.5	-	4.1
3	-	4.5	n/a	4.3	4.3	-	3.7
4	-	4.1	4.0	4.1	4.2	-	3.9
5a	-	4.3	5.0	4.3	4.6	-	4.4
5b	-	4.5	n/a	4.2	4.6	-	4.3
6a	-	4.5	5.0	4.0	4.4	-	4.3
6b	-	4.3	n/a	4.1	5.0	-	4.4
6c	-	3.7	5.0	3.5	5.0	-	4.3
7a	-	4.7	5.0	4.0	4.4	-	4.3
7b	-	4.3	n/a	4.2	5.0	-	4.4
7c	-	4.0	5.0	3.9	5.0	-	4.3
8	-	4.6	4.0	4.5	4.6	-	4.3
9	-	4.9	5.0	4.4	4.8	-	4.2
10a	-	5.0	n/a	4.6	4.6	-	4.6
10b	-	4.7	5.0	3.9	5.0	-	4.4
11	-	4.6	5.0	4.4	4.8	-	4.4
12	-	4.0	4.0	4.0	4.2	-	3.8
13a	-	3.2	4.0	3.5	3.8	-	3.4
13b	-	3.4	4.0	3.6	4.5	-	3.6
14	-	4.4	5.0	4.4	4.8	-	4.4

3. 1998 SFRP & GSRP EVALUATION RESPONSES

The summarized results listed below are from the 120 SFRP/GSRP evaluations received.

Associates were asked to rate the following questions on a scale from 1 (below average) to 5 (above average) - by Air Force base results and over-all results of the 1998 evaluations are listed after the questions.

1. The match between the laboratories research and your field:
2. Your working relationship with your LFP:
3. Enhancement of your academic qualifications:
4. Enhancement of your research qualifications:
5. Lab readiness for you: LFP, task, plan:
6. Lab readiness for you: equipment, supplies, facilities:
7. Lab resources:
8. Lab research and administrative support:
9. Adequacy of brochure and associate handbook:
10. RDL communications with you:
11. Overall payment procedures:
12. Overall assessment of the SRP:
13. a. Would you apply again?
    b. Will you continue this or related research?
14. Was length of your tour satisfactory?
15. Percentage of associates who experienced difficulties in finding housing:
16. Where did you stay during your SRP tour?
    a. At Home:
    b. With Friend:
    c. On Local Economy:
    d. Base Quarters:
17. Value of orientation visit:
    a. Essential:
    b. Convenient:
    c. Not Worth Cost:
    d. Not Used:

SFRP and GSRP associate's responses are listed in tabular format on the following page.

Table B-4. 1997 SFRP & GSRP Associate Responses to SRP Evaluation

	Arnold	Brooks	Edwards	Eglin	Griffis	Hanscom	Kelly	Kirtland	Lackland	Robins	Tyndall	WPAFB	average
# res	6	48	6	14	31	19	3	32	1	2	10	85	257
1	4.8	4.4	4.6	4.7	4.4	4.9	4.6	4.6	5.0	5.0	4.0	4.7	4.6
2	5.0	4.6	4.1	4.9	4.7	4.7	5.0	4.7	5.0	5.0	4.6	4.8	4.7
3	4.5	4.4	4.0	4.6	4.3	4.2	4.3	4.4	5.0	5.0	4.5	4.3	4.4
4	4.3	4.5	3.8	4.6	4.4	4.4	4.3	4.6	5.0	4.0	4.4	4.5	4.5
5	4.5	4.3	3.3	4.8	4.4	4.5	4.3	4.2	5.0	5.0	3.9	4.4	4.4
6	4.3	4.3	3.7	4.7	4.4	4.5	4.0	3.8	5.0	5.0	3.8	4.2	4.2
7	4.5	4.4	4.2	4.8	4.5	4.3	4.3	4.1	5.0	5.0	4.3	4.3	4.4
8	4.5	4.6	3.0	4.9	4.4	4.3	4.3	4.5	5.0	5.0	4.7	4.5	4.5
9	4.7	4.5	4.7	4.5	4.3	4.5	4.7	4.3	5.0	5.0	4.1	4.5	4.5
10	4.2	4.4	4.7	4.4	4.1	4.1	4.0	4.2	5.0	4.5	3.6	4.4	4.3
11	3.8	4.1	4.5	4.0	3.9	4.1	4.0	4.0	3.0	4.0	3.7	4.0	4.0
12	5.7	4.7	4.3	4.9	4.5	4.9	4.7	4.6	5.0	4.5	4.6	4.5	4.6
Numbers below are percentages													
13a	83	90	83	93	87	75	100	81	100	100	100	86	87
13b	100	89	83	100	94	98	100	94	100	100	100	94	93
14	83	96	100	90	87	80	100	92	100	100	70	84	88
15	17	6	0	33	20	76	33	25	0	100	20	8	39
16a	-	26	17	9	38	23	33	4	-	-	-	30	
16b	100	33	-	40	-	8	-	-	-	-	36	2	
16c	-	41	83	40	62	69	67	96	100	100	64	68	
16d	-	-	-	-	-	-	-	-	-	-	-	0	
17a	-	33	100	17	50	14	67	39	-	50	40	31	35
17b	-	21	-	17	10	14	-	24	-	50	20	16	16
17c	-	-	-	-	10	7	-	-	-	-	-	2	3
17d	100	46	-	66	30	69	33	37	100	-	40	51	46

4. 1998 USAF LABORATORY HSAP MENTOR EVALUATION RESPONSES

Not enough evaluations received (5 total) from Mentors to do useful summary.

5. 1998 HSAP EVALUATION RESPONSES

The summarized results listed below are from the 23 HSAP evaluations received.

HSAP apprentices were asked to rate the following questions on a scale from 1 (below average) to 5 (above average)

1. Your influence on selection of topic/type of work.
2. Working relationship with mentor, other lab scientists.
3. Enhancement of your academic qualifications.
4. Technically challenging work.
5. Lab readiness for you: mentor, task, work plan, equipment.
6. Influence on your career.
7. Increased interest in math/science.
8. Lab research & administrative support.
9. Adequacy of RDL's Apprentice Handbook and administrative materials.
10. Responsiveness of RDL communications.
11. Overall payment procedures.
12. Overall assessment of SRP value to you.
13. Would you apply again next year? Yes (92 %)
14. Will you pursue future studies related to this research? Yes (68 %)
15. Was Tour length satisfactory? Yes (82 %)

	Arnold	Brooks	Edwards	Eglin	Griffiss	Hanscom	Kirtland	Tyndall	WPAFB	Totals
# resp	5	19	7	15	13	2	7	5	40	113
1	2.8	3.3	3.4	3.5	3.4	4.0	3.2	3.6	3.6	3.4
2	4.4	4.6	4.5	4.8	4.6	4.0	4.4	4.0	4.6	4.6
3	4.0	4.2	4.1	4.3	4.5	5.0	4.3	4.6	4.4	4.4
4	3.6	3.9	4.0	4.5	4.2	5.0	4.6	3.8	4.3	4.2
5	4.4	4.1	3.7	4.5	4.1	3.0	3.9	3.6	3.9	4.0
6	3.2	3.6	3.6	4.1	3.8	5.0	3.3	3.8	3.6	3.7
7	2.8	4.1	4.0	3.9	3.9	5.0	3.6	4.0	4.0	3.9
8	3.8	4.1	4.0	4.3	4.0	4.0	4.3	3.8	4.3	4.2
9	4.4	3.6	4.1	4.1	3.5	4.0	3.9	4.0	3.7	3.8
10	4.0	3.8	4.1	3.7	4.1	4.0	3.9	2.4	3.8	3.8
11	4.2	4.2	3.7	3.9	3.8	3.0	3.7	2.6	3.7	3.8
12	4.0	4.5	4.9	4.6	4.6	5.0	4.6	4.2	4.3	4.5
Numbers below are percentages										
13	60%	95%	100%	100 %	85%	100%	100%	100%	90%	92%
14	20%	80%	71%	80%	54%	100%	71%	80%	65%	68%
15	100%	70%	71%	100 %	100%	50%	86%	60%	80%	82%

WIND VALIDATION:
INCOMPRESSIBLE TURBULENT FLOW PAST A FLAT PLATE

Greg Laskowski
Graduate Student
Department of Aeronautics and Astronautics

Stanford University
Department of Aeronautics and Astronautics
Durand Building
Stanford, CA 94305

Final Report for:
Summer Graduate Student Research Program
Arnold Engineering Development Center
Arnold AFB, Tullahoma TN

Sponsored by:
Air Force Office of Scientific Research
Bolling Air Force Base, DC

and

Arnold Engineering Development Center
Arnold Air Force Base

September 21, 1998

WIND VALIDATION:
INCOMPRESSIBLE TURBULENT FLOW PAST A FLAT PLATE

Gregory Michael Laskowski
Graduate Student
Department of Aeronautics and Astronautics
Stanford University

Abstract

The NPARC alliance has invested considerable resources in developing the WIND code: a robust, user friendly, finite-volume, structured, multi-zone, compressible flow solver with flexible chemistry and turbulence models which can be run on a variety of platforms. A validation effort was undertaken to examine the ability of the WIND code's accuracy and efficiency for incompressible turbulent flat plate flow. The validation work presented herein presents the results obtained upon conducting a grid independence study with and without wall functions and validating the different turbulence models, explicit Euler flux schemes, order of the Euler flux schemes, implicit methods, and time integration schemes. Also, results obtained in conducting 2D simulations were than compared with those obtained for 3D simulations. Overall, the different methods proved quite successful, with only slight problems observed with some of the test configurations.

WIND VALIDATION:
INCOMPRESSIBLE TURBULENT FLOW PAST A FLAT PLATE

Gregory Michael Laskowski

Introduction

It is generally believed in the CFD community that the first major breakthrough in CFD can be attributed to Murmon and Cole's solution of the Transonic Small Disturbance equations[1], which govern steady, irrotational, isentropic flow. Twenty-five years later, through the collaborative and individual efforts of academia, industry and the military, it is now possible to solve the full Navier-Stokes equations, explicit or implicit, conservative or non-conservative, with chemistry effects, on moving or stationary grids. Numerous methods and schemes have either been developed or applied in order to arrive at the solution of the full Navier-Stokes equations. These methods include, but are in no way limited to the handling of: turbulence, chemistry, Euler fluxes, time integration, convergence acceleration, matrix inversions (implicit solution), and zonal interfaces.

In recent years the NPARC alliance has been involved with the development of the WIND code, a finite volume, structured, multi-zone, compressible flow solver with flexible chemistry and turbulence[2] The code incorporates many of the schemes developed over the years which have demonstrated varying degrees of accuracy and efficiency. This paper presents results obtained in an extensive validation effort using many combinations of the different schemes/methods available within the code for incompressible turbulent flat plate flow. The numerical results are compared with experimental data obtained by Wieghardt[3] for friction coefficient and boundary layer velocity profiles. The results show that most schemes work effectively, and that efficiency (in terms of CPU time) varies based on the combination of the different methods applied in arriving at the converged solution.

Test Matrix

Eight key factors were the primary focus of this investigation (WIND defaults, which will be referred to as the "baseline" case, are depicted using [brackets]):

1). y^+ values	N/A
2). Wall functions	[OFF]
3). Turbulence models	[SST]
4). Explicit Euler flux schemes	[Roe Physical]
5). Euler flux orders	[2nd]
6). Implicit operators	[ADI]
7). Time integration schemes	[Euler]
8). Dimension (2D vs. 3D)	N/A

The strategy of this investigation will be categorized as follows:

Case 1) *WIND Version 2.55*

Starting with the same grid used in previous NPARC validation efforts and holding the number of grid points constant, y^+ values of 0.5, 1.0, 2.0, 4.0, 8.0, 16.0, 32.0, 64.0, 128.0, 256.0, and 512.0 were investigated for the "Baseline" case: wall functions [OFF], turbulence model [SST], Euler flux scheme [Roe Physical], order [2nd], implicit operator [ADI], time integration scheme [Euler], and dimension [2D].

Case 2) *WIND Version 2.55*

Starting with the same grid used in previous NPARC validation efforts and holding the number of grid points constant, y^+ values of 0.5, 1.0, 2.0, 4.0, 8.0, 16.0, 32.0, 64.0, 128.0, 256.0, and 512.0 were investigated for the "Baseline" case: wall functions [ON], turbulence model [SST], Euler flux scheme [Roe Physical], order [2nd], implicit operator [ADI], time integration scheme [Euler], and dimension [2D].

Case 3) *WIND Version 2.55*

Using the $y^+ = 1.0$ grid with wall functions [OFF] and holding the explicit Euler flux scheme [Roe Physical], order [2nd], implicit operator [ADI], time integration scheme [Euler], and dimension [2D] fixed, the different **TURBULENCE MODELS** were studied, namely:

a). SST
b). Spalart-Allmaras[4]
c). Baldwin-Barth[5]
d). PDT[6]
e). Baldwin-Thomas[7]

**Note: Chien k-ε was previously validated

Case 4) *WIND Version 2.43*

Using the $y^+ = 1.0$ grid with wall functions [OFF] and holding the turbulence model [SST], order [2nd], implicit operator [ADI], time integration scheme [Euler], and dimension [2D] fixed, the different explicit **EULER FLUX SCHEMES** were studied, namely:

a). Roe[8]
b). van Leer[9]
c). Coakley[10]
d). Roe Physical[11]
e). Central

Case 5) *WIND Version 2.55*

iid_table

```
function iid_table = iid_table(n, m, vare, number)

%  function iid_table = iid_table(n, m, vare, number)
%
%  Creates number test matrices which are n X m with mean 0, variance
%  var, and no x or y trend.  It returns a number X 4 matrix where the
%  first column is the minimum of the st dev  statistic for the test
%  matrix associated with the row number, the second column is the
%  mean of the st dev statistic for the test matrix associated with
%  the row number, the third column is the maximum of the st dev
%  statistic for the test matrix associated with the row number, and
%  the fourth column is the standard deviation of the the st dev
%  statistics for the test matrix associated with the row number.

for i = 1:number
   A = test_data(n,m,0,vare,0,0);
   X = sdev_stat_gen(A);
   minn = min(X);
   meen = mean(X);
   maxx = max(X);
   vari = var(X);
   variance = var(vari);
   iid_table(i,1) = min(minn);
   iid_table(i,2) = mean(meen);
   iid_table(i,3) = max(maxx);
   iid_table(i,4) = (variance)^.5;
end
```

Using the y^+ = 1.0 grid with wall functions [OFF] and holding the turbulence model [SST], explicit Euler flux scheme [Roe], implicit operator [ADI], time integration scheme [Euler], and dimension [2D] fixed, the different **EULER FLUX ORDERS** were studied, namely:

a). First-order
b). Second-order
c). Third-order
d). Central
e). Mixed fully upwind and central
f). Third-order fully upwind
g). Fourth-order upwind-biased
h). Fourth-order central
i). Fifth-order upwind biased

Case 6) *WIND Version 2.55*

Using the y^+ = 1.0 grid with wall functions [OFF] and holding the turbulence model [SST], explicit Euler flux scheme [Roe Physical], order [2nd], implicit operator [ADI] and dimension [2D] fixed, the different **TIME INTEGRATION SCHEMES** were studied, namely:

a). ADI
b). Gauss-Seidel line relaxation
c). Jacobi point iterative method

Case 7) *WIND Version 2.55*

Using the y^+ = 1.0 grid with wall functions [OFF] and holding the turbulence model [SST], explicit Euler flux scheme [Roe Physical], order [2nd], implicit operator [ADI] and dimension [2D] fixed, the different **TIME INTEGRATION SCHEMES** were studied, namely:

a). Euler
b). 3 Stage Runge-Kutta
c). 4 Stage Runge-Kutta

Case 8) *WIND Version 2.74*

For the "baseline" case a 3D simulation was conducted. The 3D grid consisted of five planes spaced $\Delta z = 0.5$" apart, where each plane consisted of the same x and y data points used in Case 1) - Case 5). The **3D INDEX SEQUENCING** was investigated in order to determine its' effect on overall efficiency and performance (CPU time).

a). ijk sequencing
b). jki sequencing
c). kij sequencing

The experimental data of Wieghardt[3], namely skin friction coefficient and boundary layer velocity profiles, was used to assess the numerical results of the validation cases presented herein. The flow conditions reported by Wieghardt, and used in the numerical simulations, are presented in Table 1.

Table 8-1. Flow conditions

Total Pressure (psia)	Static Pressure (psia)	Total Temperature (R)	Static Temperature (R)	Mach Number	Reynolds Number (/ft)
15.1	14.7	534.0	530.0	0.2	1.38×10^6

Computational Grids

The initial 2D computational grid selected for this investigation was the same as that used in the NPARC validation efforts, and is depicted in Figure 8-1. The grid consists of 126 grid points in the streamwise direction and 76 grid points in the transverse direction. The grid shown in Figure 8-1 is packed near the wall, with approximately 51 points placed within the boundary layer while maintaining $y^+ = 1.0$.

A grid refinement study was also conducted (Case 1). Maintaining the same number of grid points in the streamwise and transverse directions, y^+ values of 0.5 - 512.0 (successively doubling y^+, see Case 1 description) were investigated.

3D simulations were also conducted for $y^+ = 1.0$. The 3D grid consisted of five planes spaced $\Delta z = 0.5$" apart, where each plane consisted of the same x and y data points used in Case 1) - Case 5).

Boundary Conditions

The *.cgd files, which contain the grid data and boundary condition information, were created using GRIDGEN and Gman. Along the i = 1 boundary, the "FROZEN" boundary condition was invoked and the Mach number (0.2), total pressure (15.1157 psia), total temperature (523.152 R), angle of attach (0), and side slip angle (0), were specified. Along the i = imax boundary, the "CONFINED OUTFLOW" boundary condition was implemented. Along the j = 1 boundary, the "INVISCID WALL" condition was invoked for i = 1 - 25, whereas the "VISCOUS WALL" condition was specified for i = 26 - 126. Finally, along the j = jmax boundary, the "INFLOW/OUTFLOW" condition was used.

For the 3D case ijk sequencing, the above is still true where the i and j lines are now i and j constant planes. For the k = 1 plane and k = kmax plane, the reflection boundary condition was specified.

Convergence

For each case investigated, a CFD number of 10 was initially chosen. The solution was advanced and considered converged when the residual began to plateau (see Figure 8-2). The CFL condition was

than incremented by 10, the flowfield reinitialized to freestream conditions, and the solution advanced. If the solution proved stable, the CFL number was then incremented further and the process repeated until the maximum CFL number was determined. Thus, the maximum allowable CFL condition for each case was determined, and convergence was guaranteed. It was determined that only the RHS operator had an effect on the maximum CFL number that could be used. It should be noted that only the Roe and Roe physical schemes allowed CFL numbers greater than 10, in fact one order magnitude higher than the other schemes investigated.

Results

Figure 8-3 shows the predicted friction coefficient and velocity profiles at 5 "i" locations obtained using both the NPARC and WIND codes. In this particular case, the explicit flux operator [CENTRAL], implicit operator [ADI], Euler flux order [2nd], and grid [i = 256, j = 76, and $y^+ = 1.0$] are the same, and the turbulence models are similar [SST for WIND (which is a mixed k-ω formulation in the boundary layer and k-ε formulation in the freestream) and Chein k-ε model for NPARC]. In terms of the friction coefficient, the figure shows that the results obtained with WIND are in much closer agreement with the experimental data than was obtained using the NPARC code. However, at the i = 32 location, which is near the plate leading edge, the opposite is true. Note that as the velocity profile develops, the numerical results obtained using the two codes are nearly indistinguishable, and both sets of results are in very good agreement with the experimental data.

Case 1) Figure 8-4 shows the numerical results obtained using the WIND code in terms of the friction coefficient and velocity profiles at 5 "i" locations for the different y^+ grids. It can be seen that y^+ values up to about 4.0 yield good results when compared to the experimental data. As the value of y^+ increases, the first grid point near the wall moves out of the viscous sublayer and the assumptions the various transport turbulence models are based on become invalid. Figure 8-4 also shows the variation of y^+ with Reynold's number. Notice that y^+ does vary somewhat from the plate leading edge to the trailing edge.

Case 2) Figure 8-5 compares the effect of y^+ with and without wall functions. As can be seen in the figure, the wall function allows for much larger values of y^+ while still yielding fairly accurate results. Note that near the plate leading edge, a kink is evident. For $y^+ = 256.0$ it occurs at $Re = 0.8 \times 10^6$, at $y^+ = 64.0$ it occurs at $Re = 1.2 \times 10^6$, and at $y^+ = 32.0$ it occurs at $Re = 2.8 \times 10^6$. This can most likely be attributed to the fact that y^+ is not constant along the plate surface, as was depicted in Figure 8-5. As y^+ increases with Reynolds number, points are pulled out of the viscous sublayer and the wall functions at which point the wall functions are switched on.

Case 3) Figure 8-6 displays the results obtained using different turbulence models while maintaining everything else the same. Excellent agreement among most of the different turbulence models and Wieghardt's data can be observed in terms of the friction coefficient. There is also good agreement in terms of the velocity profile except, perhaps, for i = 32, near the plate leading edge. There

does appear to be a problem with the Baldwin-Barth model. It severely underpredicts the friction coefficient and seems to lack sufficient dissipation near the outer edge of the boundary layer. This is an indication of a possible bug in the code.

Case 4) Figure 8-7 presents the results obtained using the different RHS operators. Again, excellent agreement between the numerical results and the experimental data is observed in terms of the friction coefficient (note that the van Leer data is not seen in this plot). It seems that the only discrepancy exists near the plate leading edge, as was observed in Case 5. While the central scheme is too dissipative, the Roe scheme is lacking in sufficient dissipation. Note that the van Leer schemes produces poor results at each i location, indicating a possible bug in the code.

Case 5) Figure 8-8 presents the results obtained using the different RHS orders. Note that it was determined that the third order fully upwind order was not functioning correctly. The code terminated the first iteration for no apparent reason. Other than 3U, all other orders produced excellent results as can be seen in the figure.

Case 6) In this case, not only was the accuracy of interest, but the time required for convergence as well. Figure 8-9 presents the results obtained using the different implicit operators. As can be seen in Figure 8-9, there is little, if any, discernible difference between the different numerical results. However, as can be seen in Figures 8-10, the time required for such solutions varies greatly. While Figure 8-10 assures that the convergence rate is identical for the 3 different implicit operators, the time required for convergence is much lower for the ADI scheme than the 2 iterative methods. Note, furthermore, that the approximate factorization error of the ADI scheme, does not have a noticeable effect on any of the results obtained for this particular case.

Case 7) As with Case 6, this case was also concerned with the efficiency of the different numerical methods as well with the accuracy of the results. Figure 8-11 shows that no discernible difference exists in terms of the friction coefficient and velocity profiles. However, it was determined that the Euler scheme proved to be more than 50% faster than the 3 stage Runge Kutta scheme and nearly 70% faster than the 4 stage Runge Kutta scheme. For a steady state problem, it is quite obvious that the order accuracy is not nearly as important as the time require for convergence.

Case 8) As a final test of the WIND code, some 3D simulations were investigated which yielded interesting results. First, the sequencing of the indicies was varied to determine which resulted in the fastest convergence. Figure 8-12 shows that, in terms of the friction coefficient, there exists no difference between the different planes and different sequencing. Note, however, that the 3D friction coefficient is higher than the 2D friction coefficient, keeping all numerical schemes/methods the same. Also, note the "kink" that exists near $Re = 5.0 \times 10^6$. Figure 8-13 presents the CPU requirements for the different sequencing. It can be seen that the jki sequencing is approximately 3% faster than the ijk sequencing and nearly 6% faster than the kij sequencing. Figure 8-14 presents the convergence rates for the different

sequencing, allowing one to conclude that the same number of iterations are required for convergence and that the results presented in Figure 8-13 is in fact an accurate assessment of efficiency.

It was hypothesized that the "kink" seen in Figure 8-12 could possibly be attributed to the turbulence model (SST). As such, a case was also investigated using the PDT and Spalart-Allmaras turbulence models, and the 3D results compared with the 2D results. First, in looking at Figure 8-15, note that convergence appears to occur much faster using the algebraic model than the 2 transport models, and that the 1 equation model appears to converge slightly faster than the 2 equation model, as one would expect. However, looking at the results presented in Figure 8-16, it can be seen that the Spalart-Allmaras model yields the best agreement when comparing 2D and 3D results. Also, the "kink" is no longer apparent. Finally, it seems that there is a problem with the PDT model in that the friction coefficient appears almost laminar. There is, at present, no explanation why the 2D and 3D simulations differ when changing the different turbulence models.

Conclusions

A validation effort using the WIND code to solve for incompressible turbulent flow past a flat plate was conducted. The results show that most numerical methods and schemes work effectively with the exception of: the Baldwin-Barth turbulence model, the 3rd Order fully upwind order for the RHS operator, and the van Leer RHS operator. It was observed that efficiency (defined as the number of iterations per CPU second) more than accuracy varies depending on the combination of the different schemes/methods for this simple test case. It would be interesting to conduct this same investigation, using the same test matrix, for a slightly more complicated test case where shocks, shear layers and separation are present. Only than can one conclude the best combination of schemes/methods to be used for a particular case.

Acknowledgments

This work was supported by the AFOSR program during the summer of 1998 and was carried out at the Arnold Engineering Development Center in Tullahoma, Tennessee. On a personal note, the author would like to especially thank Dr. Greg Power, Dr. Ken Tatum, Dr. Chris Nelson, and Dr. Mark Underwood at AEDC for their assistance in running the WIND code and in analyzing the results.

References

1. Murmon, E. M., Cole, J. D., "Calculation of Plane Steady Transonic Flows," AIAA Journal, vol. 9, pp. 114-121.

2. Bush, R. H., Power, G. D., Towne, C. E., "WIND: The Production Flow Solver of the NPARC Alliance," AIAA Paper 98-0935, January, 1998.

4. Spalart, P. R., Allmaras, S. R., "A One-Equation Turbulence Transport Model for Aerodynamic Flows," AIAA Paper 92-0439, 1992.

5. Baldwin, B. S., Barth, T. J., "A One-Equation Turbulence Model for High Reynolds Number Wall-Bounded Flows," NASA TM-102847, 1990.
6. Thomas, P. D., "Numerical Method for Predicting Flow Characteristics and Performance of Nonaxisymmetric Nozzles-Theory," Langley Research Center, NASA CR 3147, 1979.
7. Baldwin, B. S., and Lomax. H., "Thin Layer Approximation and Algebraic Model for Separated Turbulent Flows," AIAA Paper 78-257, 1978.
8. Roe, R. L., "Approximate Riemann Solvers, Parameter Vectors, and Difference Schemes," Journal of computational Physics, VOL. 43, pp. 357-372.
9. van Leer, B., Thomas, J. L., Roe, P. L., and Newsome, R. W., "A Comparison of Numerical Flux Formulas for the Euler and Navier-Stokes Equations," AIAA Paper 87-1104, 1987.
10. Coakley, T. J., "Implicit Upwind Methods for the Compressible Navier-Stokes Equations," NASA TM- 84364, 1983.
11. Cain, A. B. and Bush, R. H., "Numerical Wave Propagation Analysis for Stretched Grids," AIAA Paper 94-0172, 1994.

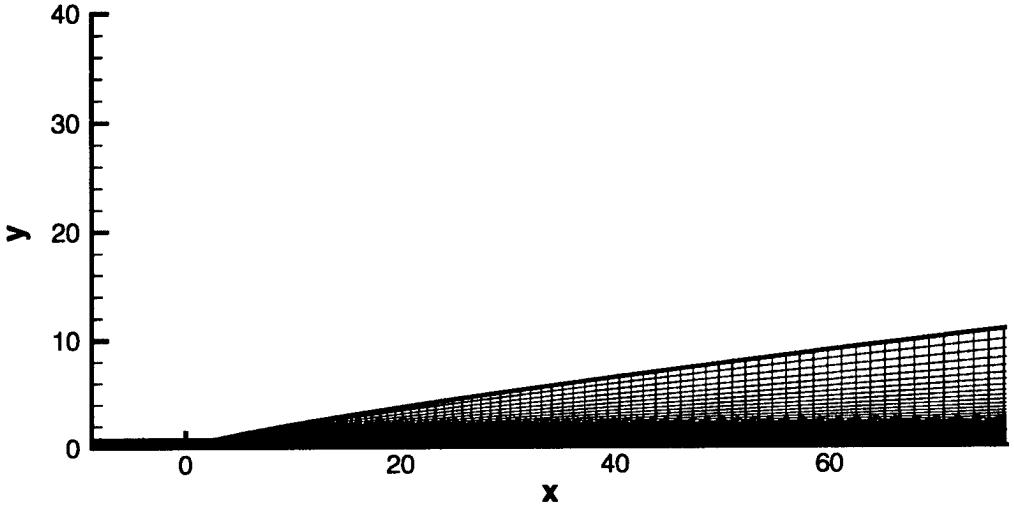

Figure 1: Computational grid

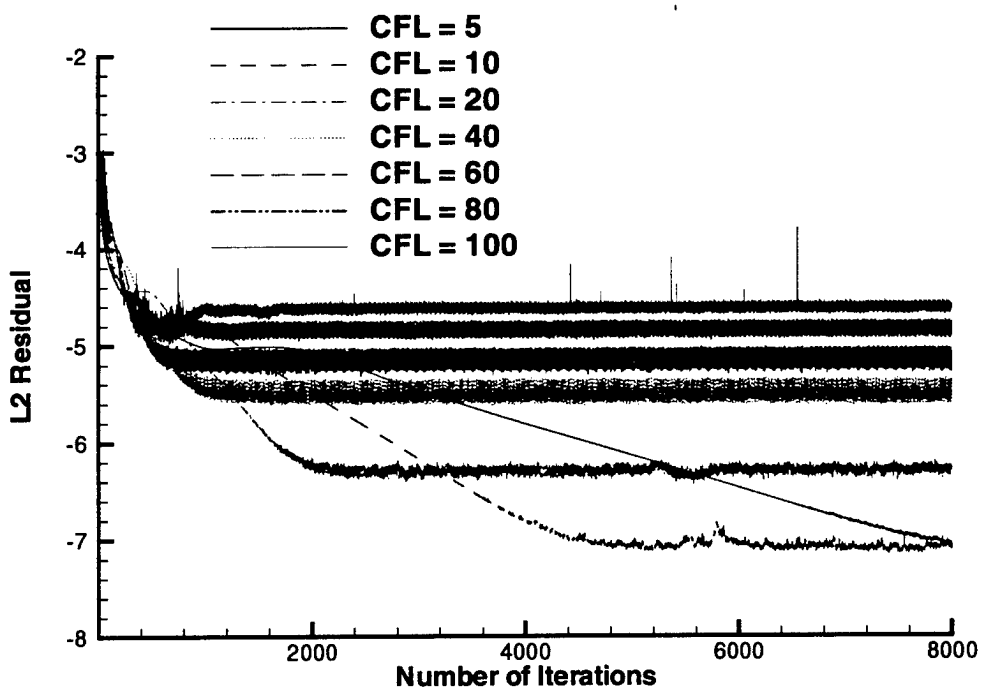

Figure 2 Effect of CFL on convergence

Incompressible Flow Past a Flat Plate: M = 0.2, Re = 1.03×10^7

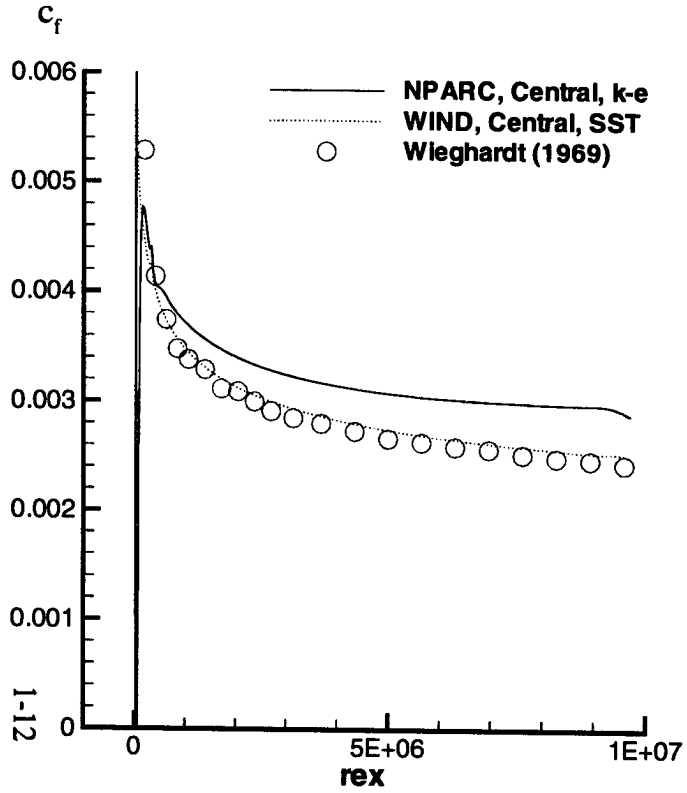

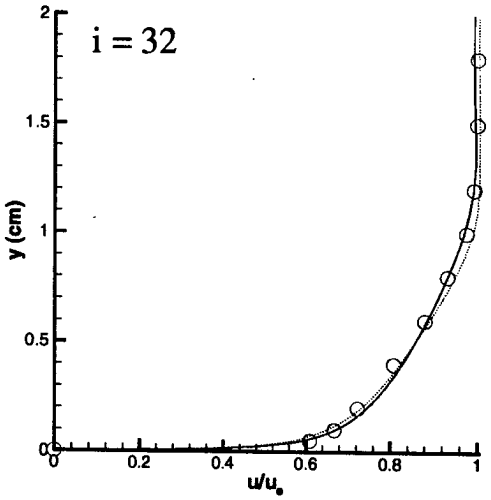

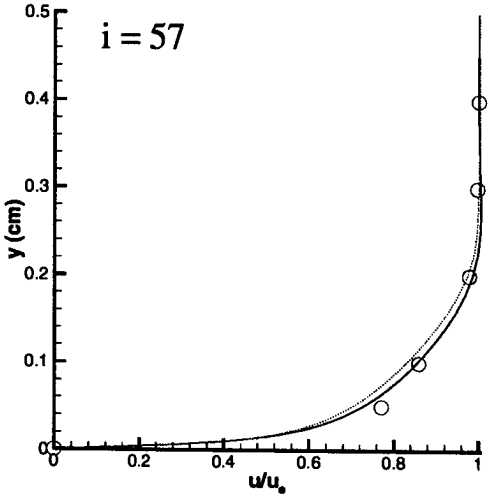

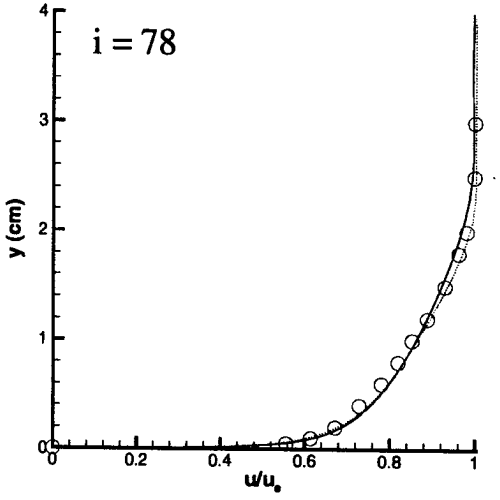

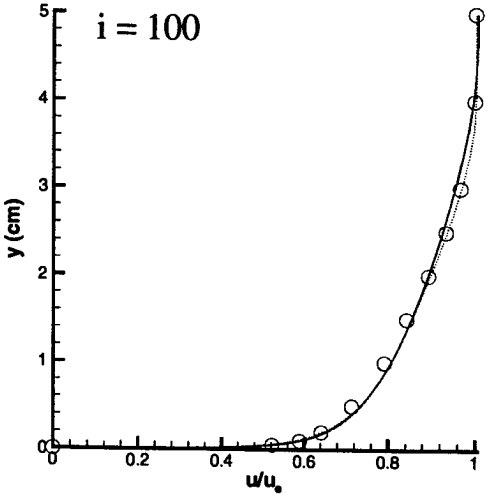

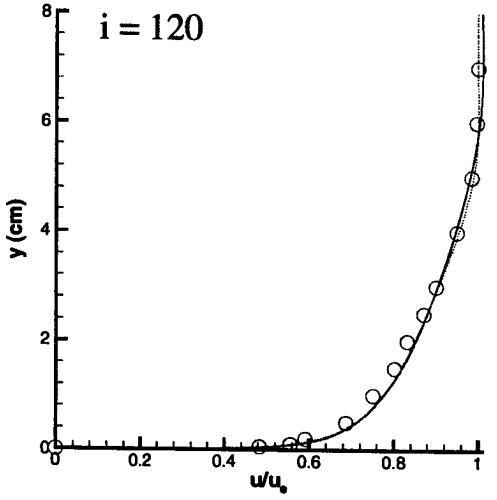

Figure 3 Comparison of NPARC and WIND results

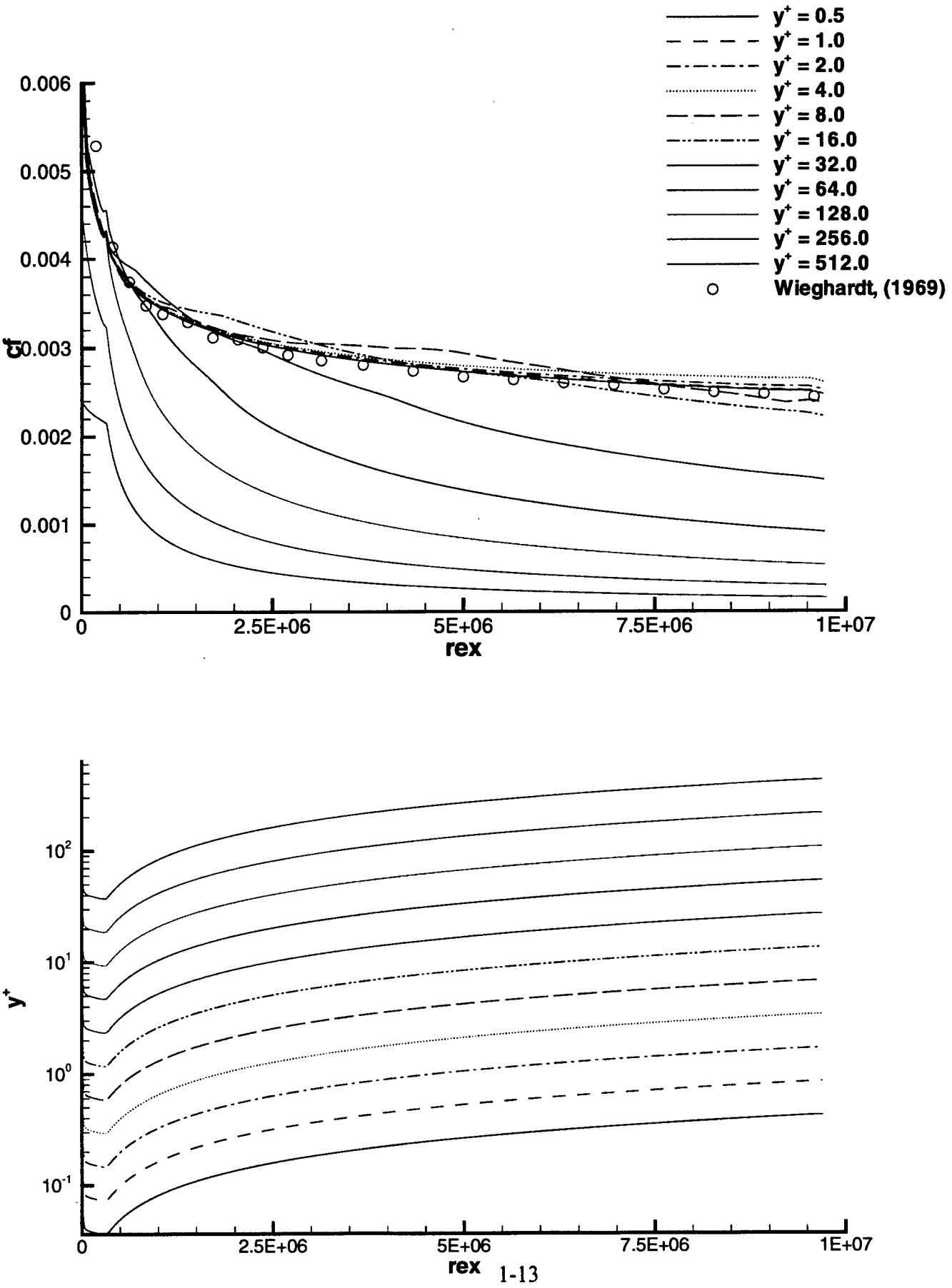

Figure 4 Effect of y+ on friction coefficient

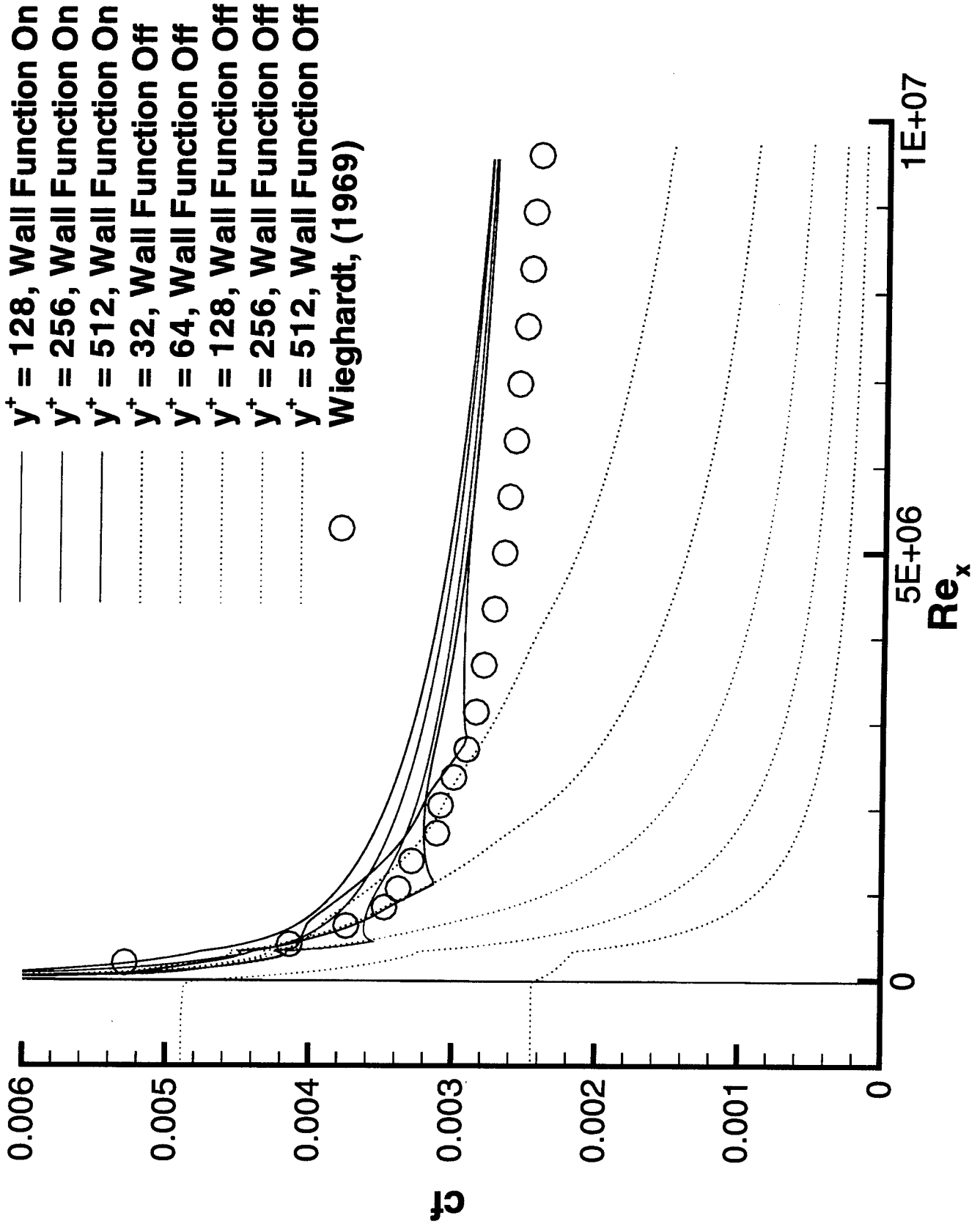

Figure 5 Effect of wall functions

Incompressible Flow Past a Flat Plate: M = 0.2, Re = 1.03 x 10^7

Comparison of Turbulence Models; Roe Physical 2nd, ADI

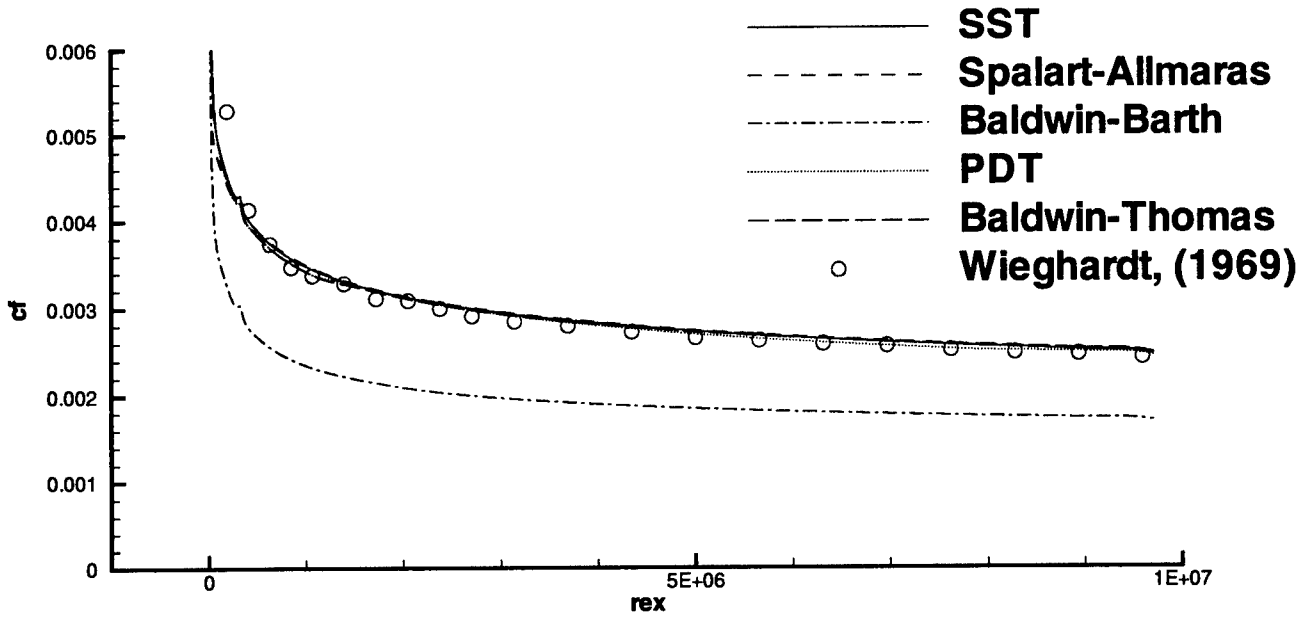

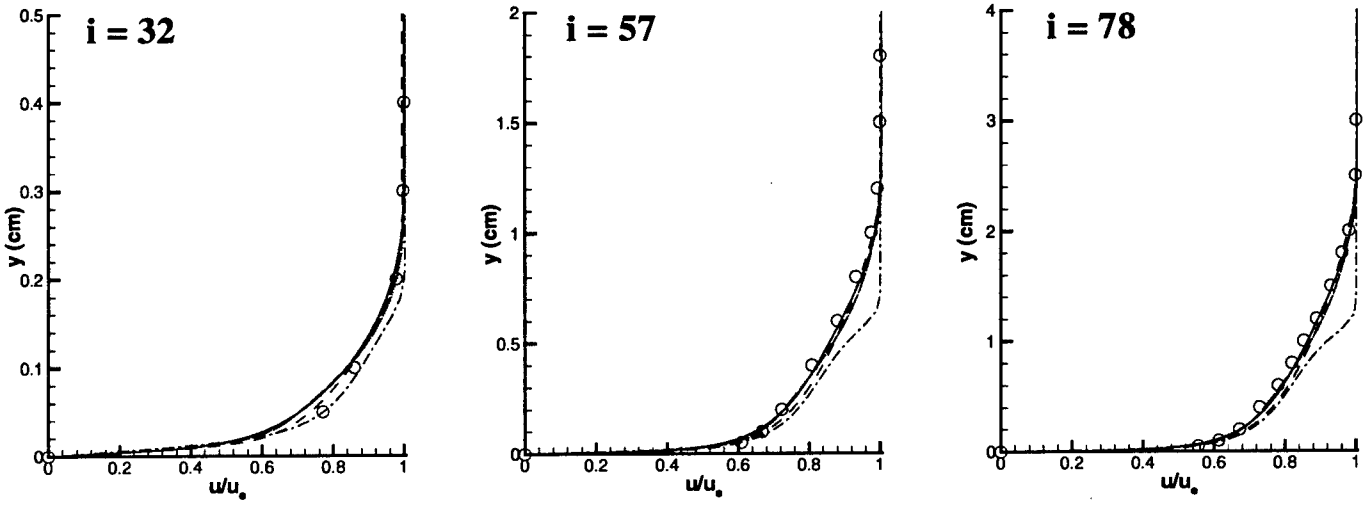

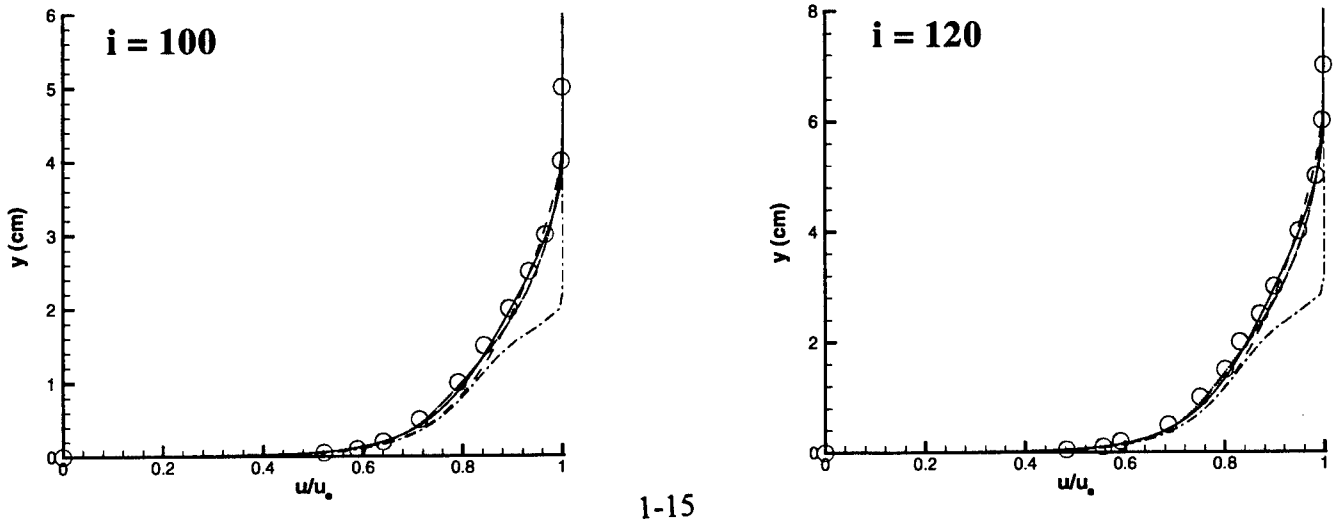

Figure 6 Effect of turbulence nodels

Incompressible Flow Past a Flat Plate: M = 0.2, Re = 1.03 x 10^7

Comparison of Explicit Flux Operators, 2nd Order, SST Turbulence Model, ADI

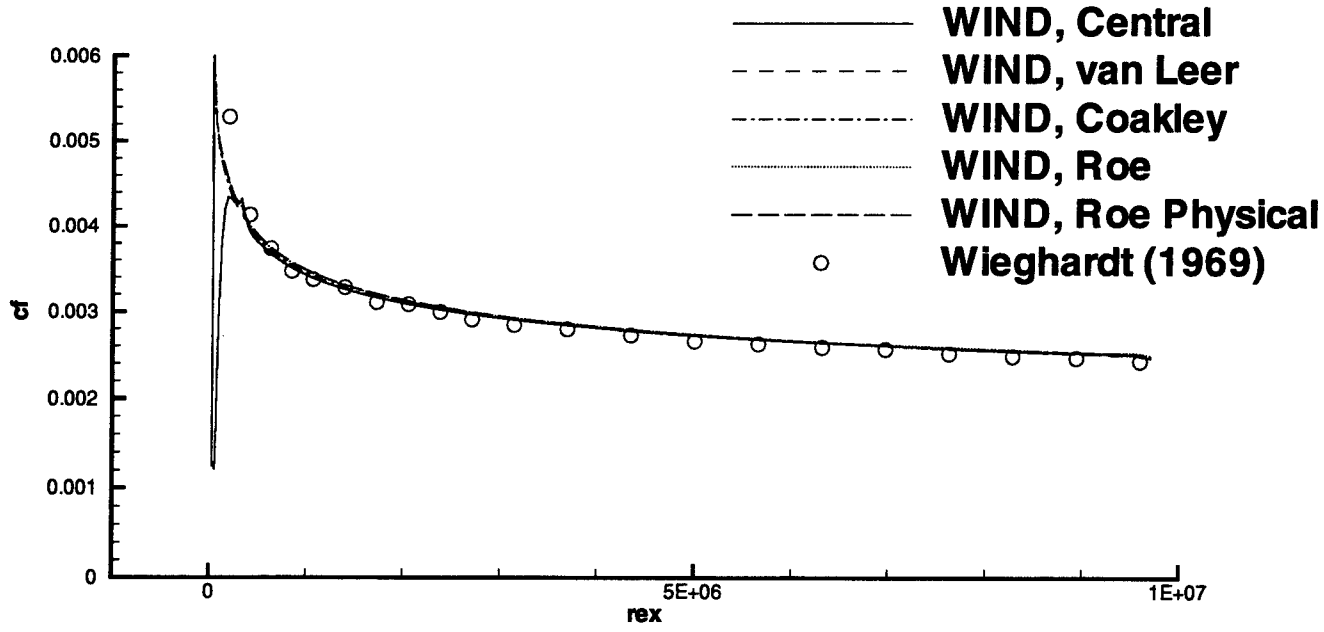

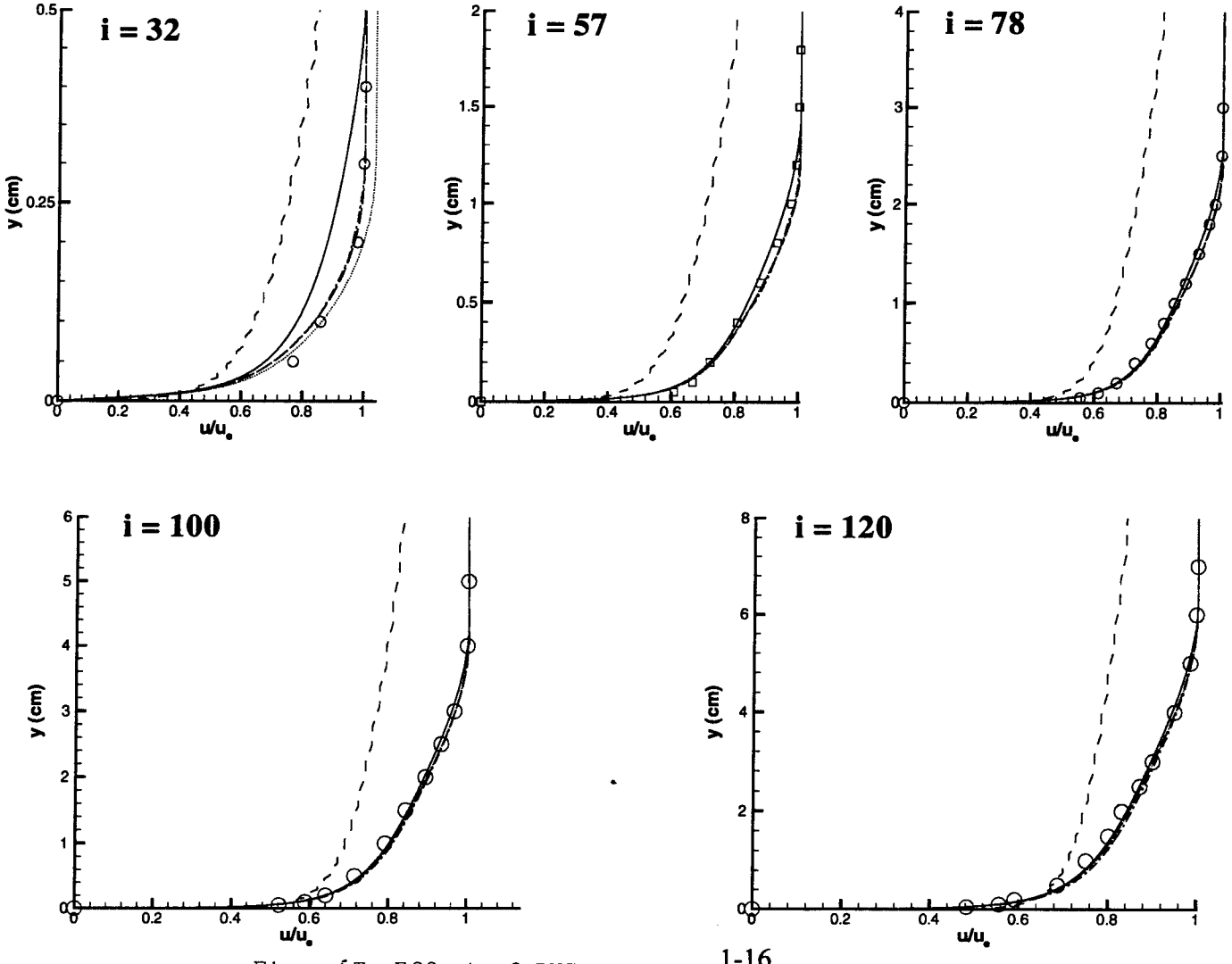

Figure 7 Effect of RHS operator

Incompressible Flow Past a Flat Plate: M = 0.2, Re = 1.03×10^7

Comparison of Explicit Flux Operator ORDER. Roe Scheme. SST Turbulence Model. ADI

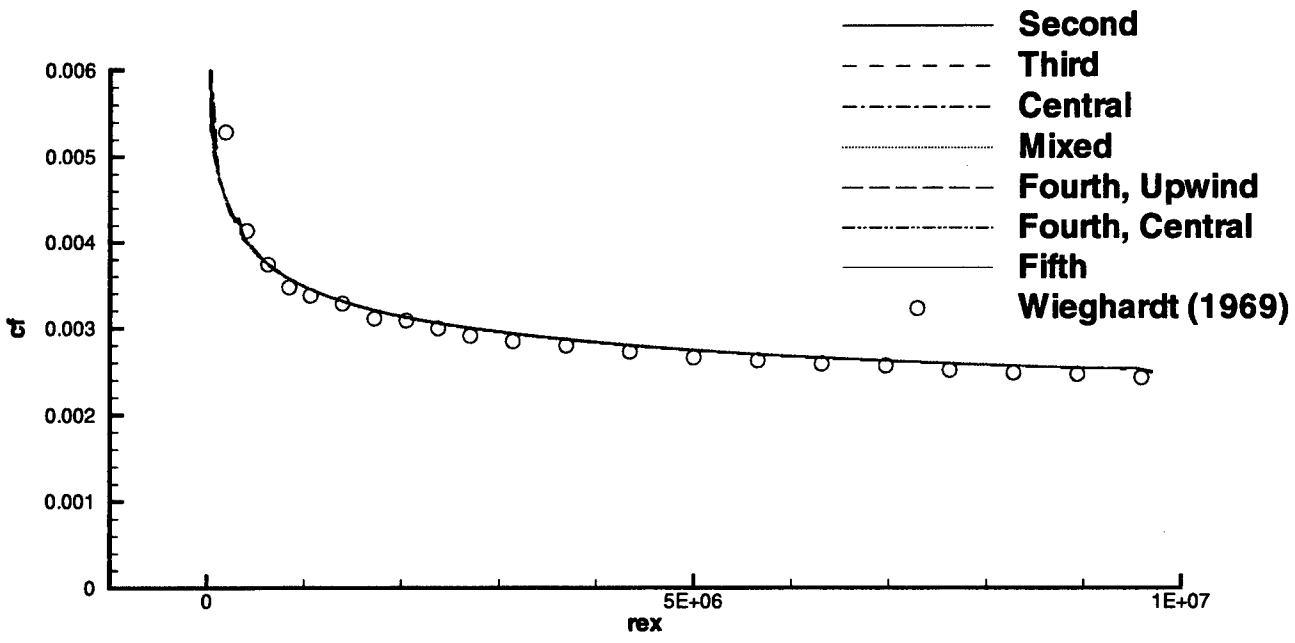

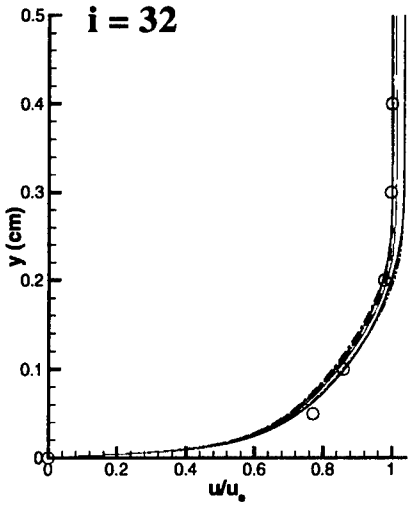

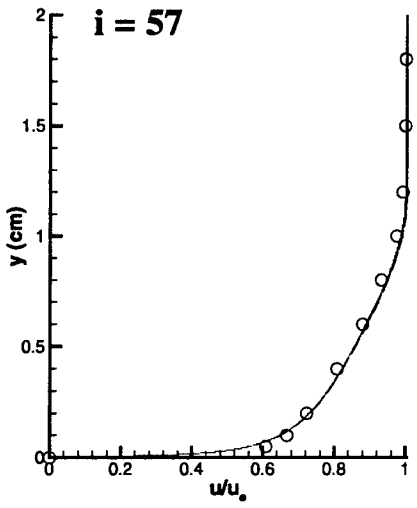

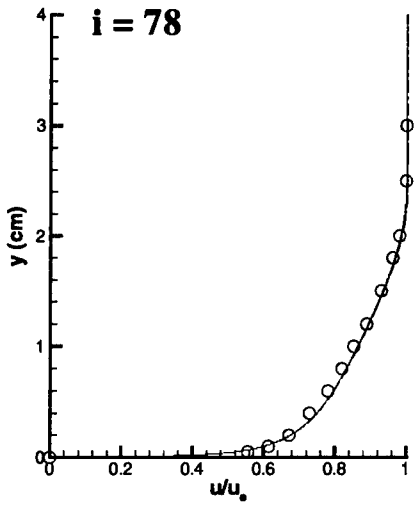

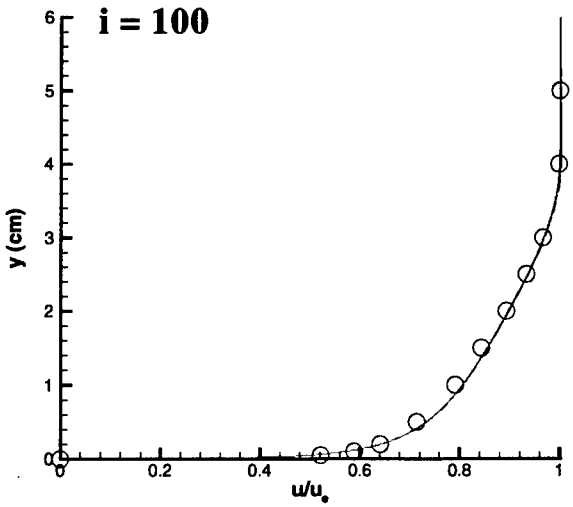

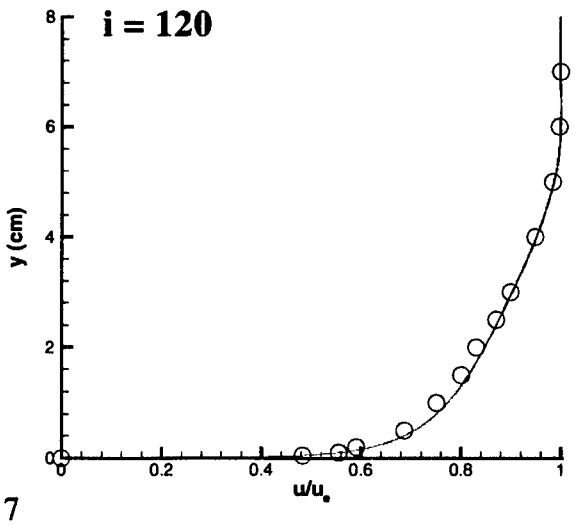

Figure 8 Effect of RHS order

Incompressible Flow Past a Flat Plate: M = 0.2, Re = 1.03 x 10^7

Comparison of Implicit Operators, SST Turbulence Model, Roe Physical 2nd, ADI

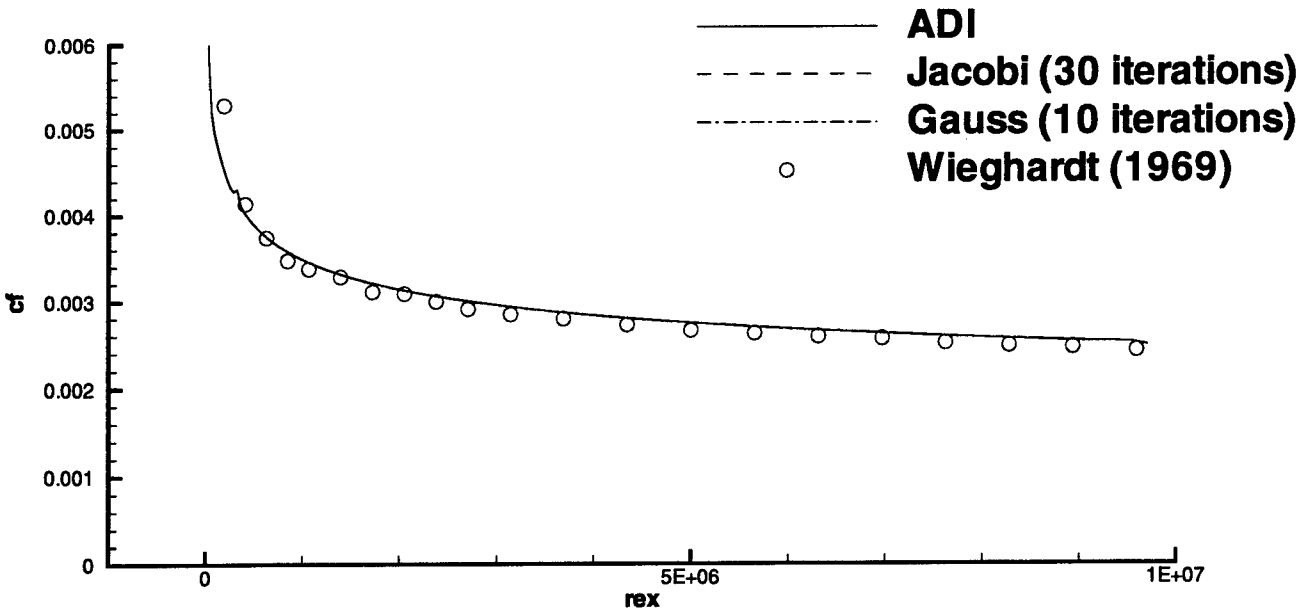

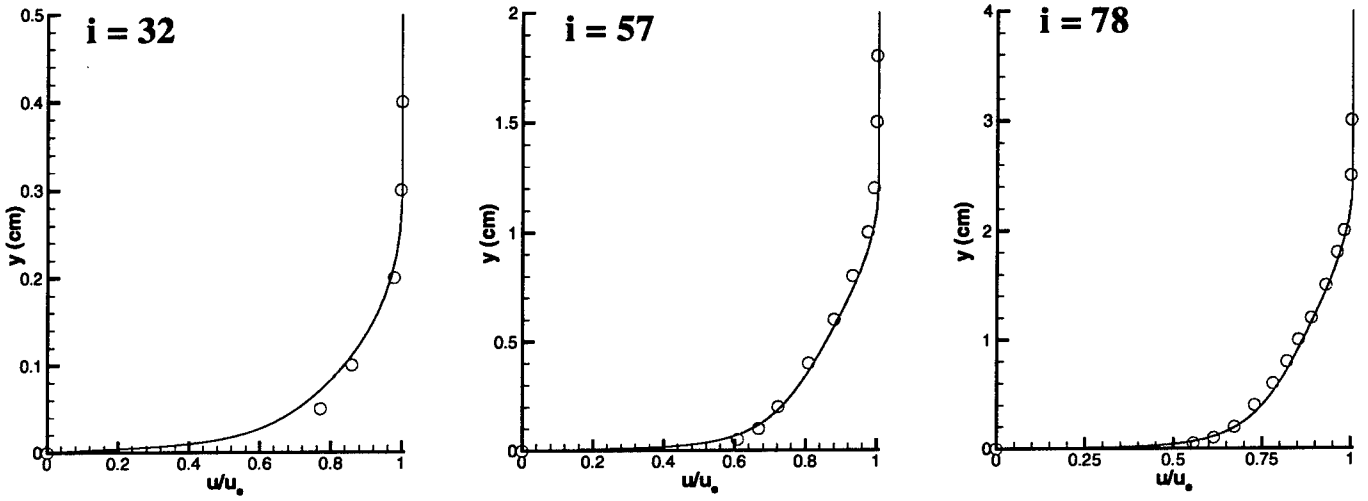

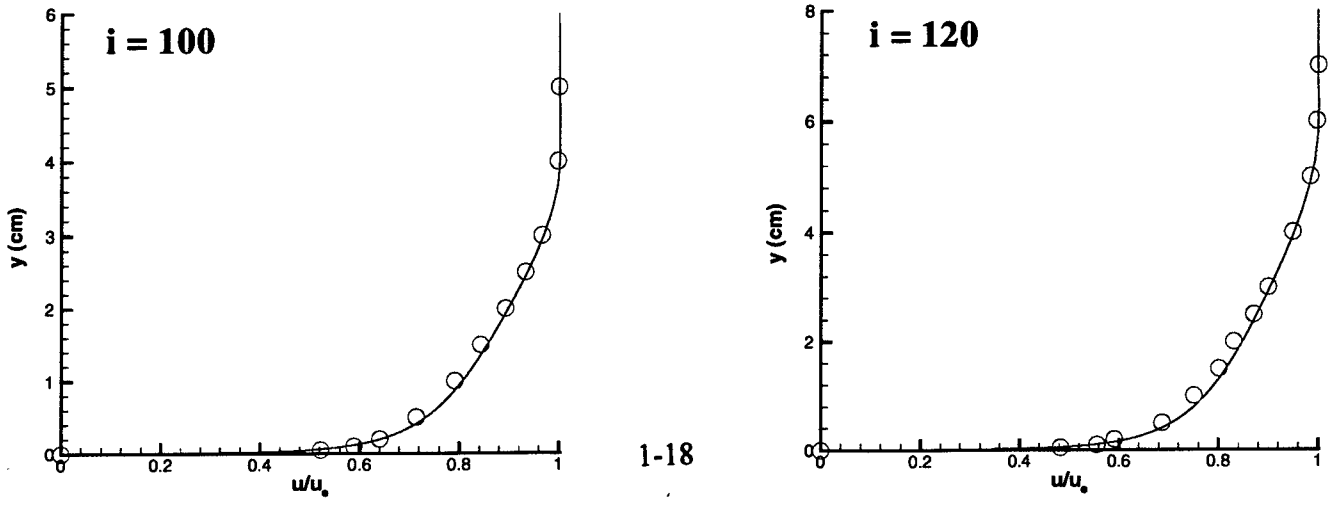

Figure 9 Effect of implicit methods

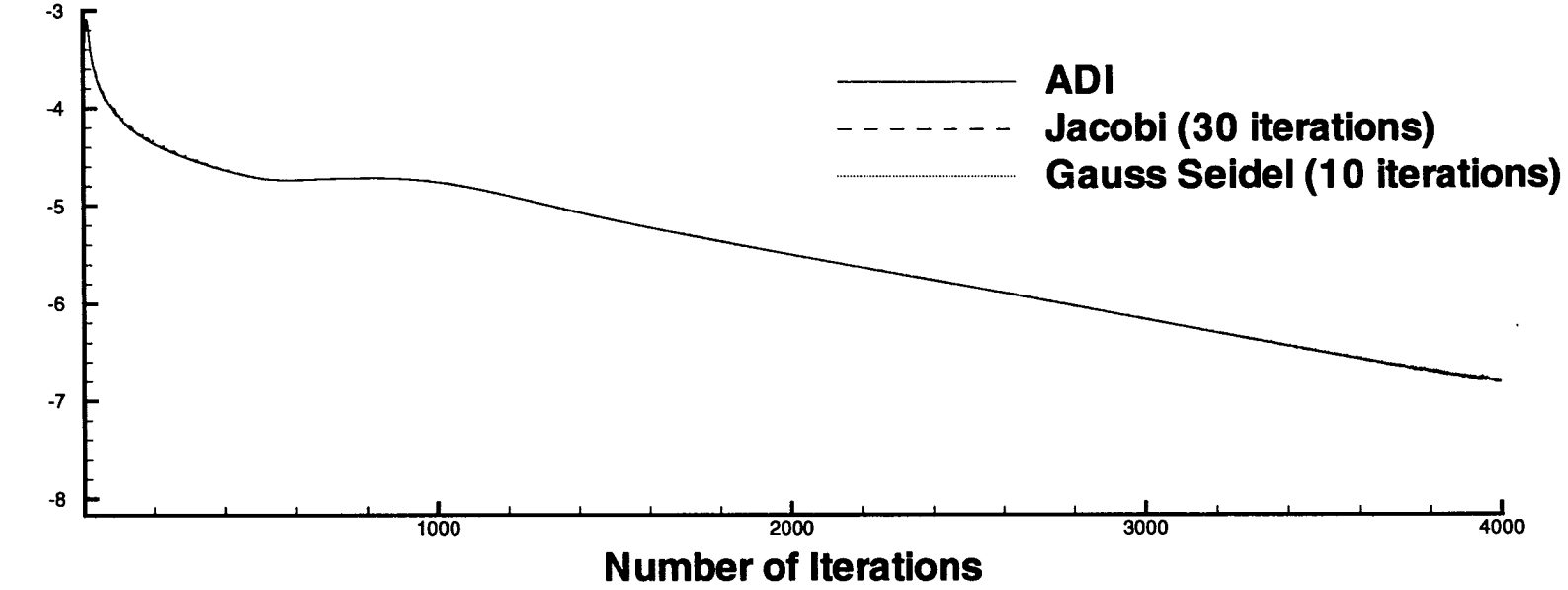

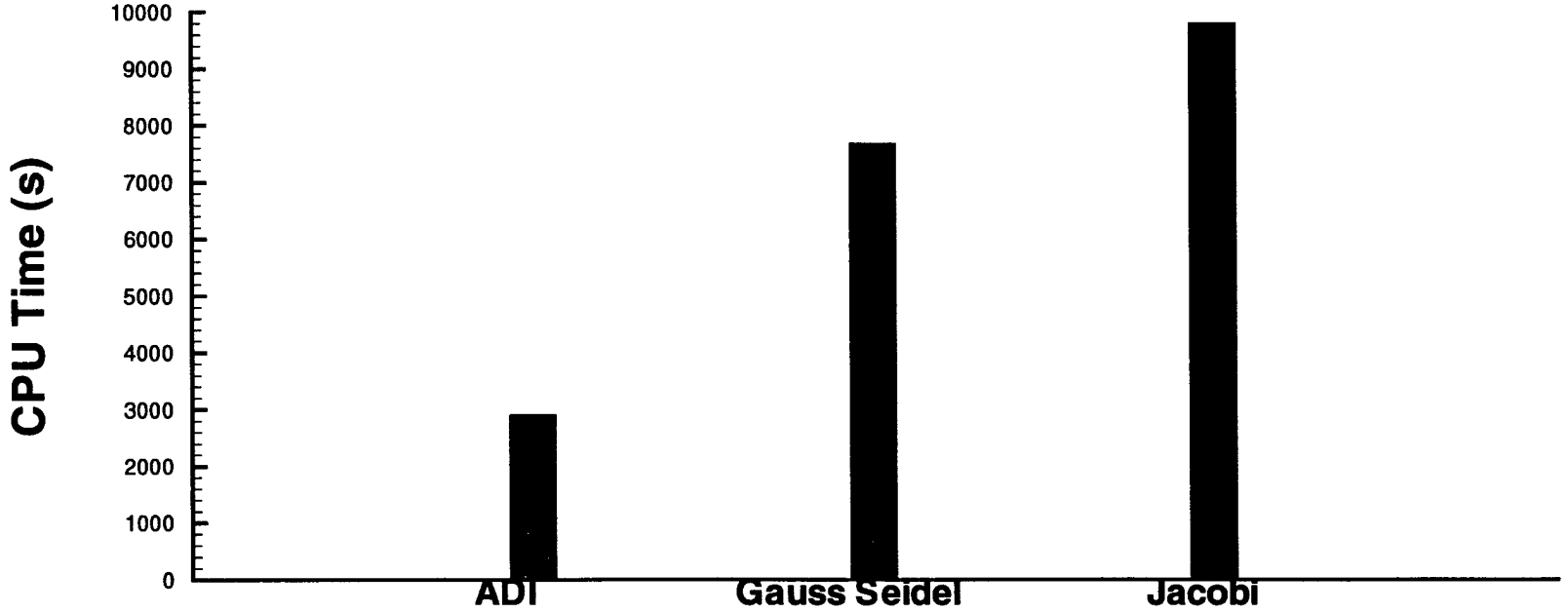

Figure 10 Efficiency of implicit methods

Incompressible Flow Past a Flat Plate: M = 0.2, Re = 1.03 x 10^7

Comparison of Time Integration Schemes, SST Turbulence Model, Roe Physical 2nd, ADI

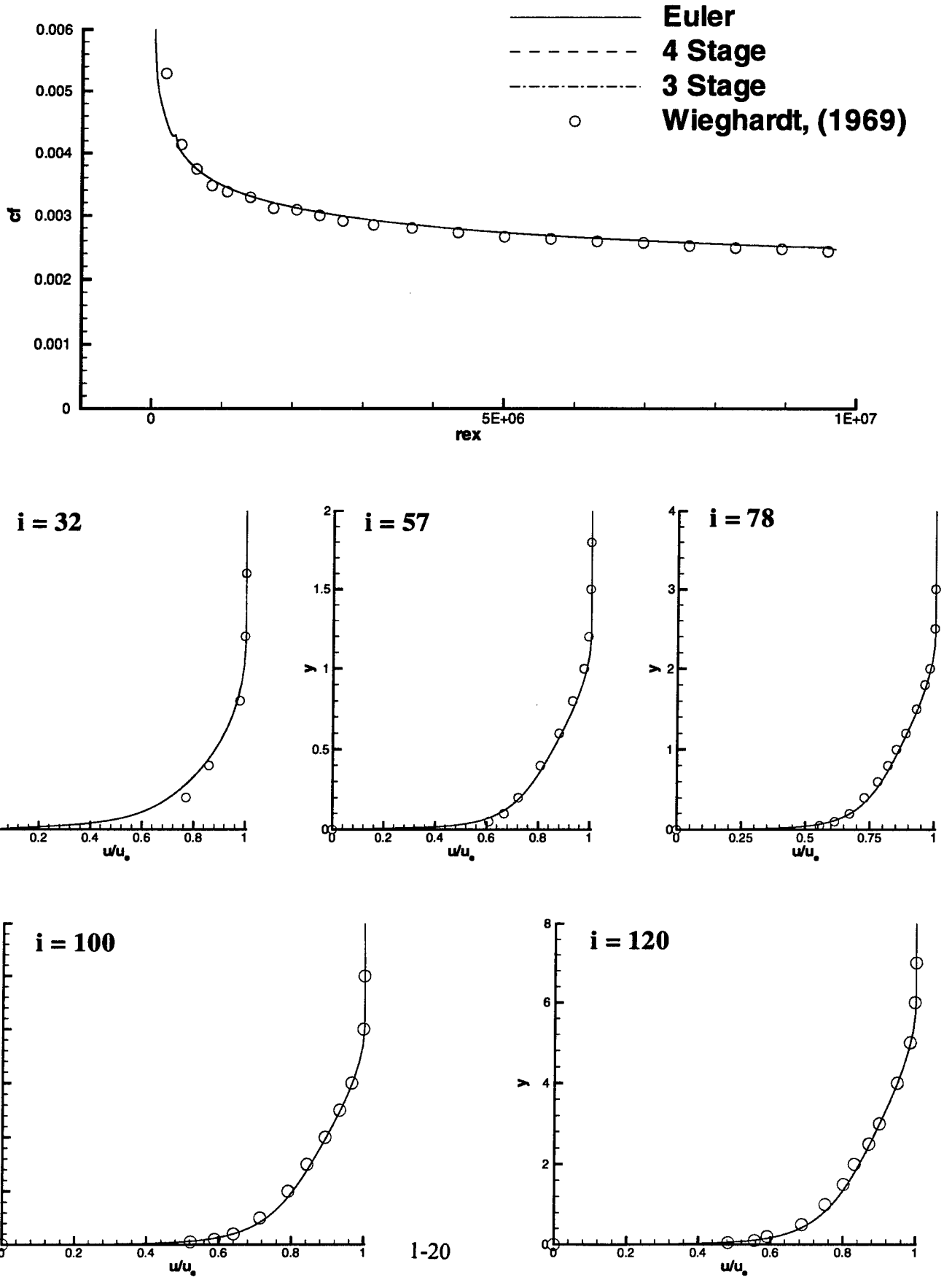

Figure 11 Effect of time integration schemes

RELATIONSHIP BETWEEN GROWTH HORMONE AND MYELIN BASIC PROTEIN EXPRESSION *IN VIVO*

Donna M. Lehman
Graduate Student
Department of Cellular and Structural Biology

The University of Texas Health Science Center at San Antonio
7703 Floyd Curl Drive
San Antonio, Texas 78284

Final Report for:
Graduate Student Research Program
Clinical Investigations Division, Wilford Hall

Sponsored by:
Air Force of Office of Scientific Research
Bolling Air Force Base, DC

and

Wilford Hall

September 1998

RELATIONSHIP BETWEEN GROWTH HORMONE AND MYELIN BASIC PROTEIN EXPRESSION *IN VIVO*

Donna M. Lehman
Graduate Student
Department of Cellular and Structural Biology
The University of Texas Health Science Center at San Antonio

ABSTRACT

Proper functioning of the mammalian nervous system requires myelination of neuronal axons. Myelination of the newborn mouse brain begins shortly after birth and is complete by about 20 days of age. Abnormalities of myelin basic protein (MBP) production have a direct impact on myelination as has been demonstrated in the shiverer mouse. Mice with less than 25% of normal MBP levels have aberrant myelination and brain development and demonstrate a characteristic tremor at 12 days of age. Growth hormone (GH) and insulin-like growth factor I (IGF-1) have been shown *in vitro* and *in vivo* to affect myelination. This project explores the effect of GH deficiency on myelin basic protein expression to determine whether GH deficiency exacerbates MBP haploinsufficiency. These studies grew out of studies undertaken on children with 18q- syndrome who have only a single copy of the MBP gene, are hypomyelinated, and are also shown to suffer growth hormone deficiency or insufficiency. A hybrid mouse model that mimics these deficiencies of 18q- patients was developed to explore the relationship between GH and MBP *in vivo*.

RELATIONSHIP BETWEEN GROWTH HORMONE AND MYELIN BASIC PROTEIN EXPRESSION *IN VIVO*

Donna M. Lehman

INTRODUCTION

Expression of the myelin basic protein (MBP) gene is critical for normal myelination of the central nervous system (CNS). This has been most clearly demonstrated by the neuropathology of the mutant shiverer (*shi/shi*) mouse in which a large portion of the MBP gene is deleted and MBP protein is essentially undetectable (1,2). Consequently, the CNS has virtually no compact myelin. These mutants exhibit a characteristic tremor (shiver) appearing at 12 days of age, coincident with the normal age at which myelination occurs in rodents, and die prematurely usually during status epilepticus. That MBP deficiency is responsible for the phenotype is supported by mutant rescue with a MBP transgene (3).

Cross-breeding experiments utilizing mice transgenic for the MBP gene have established the level of MBP expression sufficient for normal myelinogenesis (4). Heterozygous shiverer mice produce about 50% of the normal level of MBP mRNA and a proportionate amount of MBP protein. These animals exhibit a normal behavioral and morphological phenotype; however, they have minor biochemical changes in myelin composition. Mice which express less than 25% of MBP display the shivering of the dysmyelinating phenotype. These data indicate that the level of MBP expression influences the assembly of myelin by oligodendrocytes which suggests that factors which influence MBP expression also influence myelin synthesis and assembly. Additionally, factors that regulate oligodendroglial proliferation and differentiation may affect myelinogenesis. In this regard, there is much evidence, both *in vivo* and *in vitro*, that growth hormone (GH) and insulin-like growth factor 1 (IGF-1) enhance myelination (5-10). GH-deficient mice, such as the little (*lit/lit*) mutant which has an abnormality of the GH-releasing hormone receptor (Ghrhr) (11), have been reported to be hypomyelinated and correctable by early postnatal GH treatment (12).

Based on these observations, GH may be a potentiator of MBP production. To test this, we have examined the impact of naturally occurring GH deficiency (*lit/lit*) on MBP and myelination *in vivo*, investigated the effects of MBP deficiency (*shi/shi*) on GH and IGF-1 production, and explored the

relationship between GH and MBP in a hybrid mouse (*lit/lit, +/shi*) model. We hypothesized that if GH affects MBP production, then MBP levels that are already reduced in the +/shi mouse may be further reduced in the GH-deficient hybrid, and therefore, the affected mice may display the dysmyelinating phenotype. In this case, early treatment with GH might delay or prevent the appearance of the tremor. Alterations in developmental progression of myelination and its impact on function are being investigated.

These studies in mice grew out of studies undertaken on children with 18q- syndrome (11,12,13). The characteristic features of this syndrome are short stature, mental retardation and deafness. Affected children have only a single copy of the MBP gene and are hypomyelinated as demonstrated by quantitative magnetic resonance relaxometry (16). Half of affected children are GH-deficient and the other children have evidence of dysregulation of GH production. Accumulating human data suggest that GH treatment may improve both myelination and cognitive function (unpublished) raising the possibility that a relationship exists between MBP and GH. These mouse studies permit the opportunity to more thoroughly explore the relationship between GH and MBP within the context of the developing brain and may provide insight into novel treatment approaches to children with hypomyelination.

METHODOLOGY

Mouse colony: Little and shiverer mutant mice were supplied by Jackson Laboratory. The little mutant is in the C57Bl/6J background, and the shiverer mutant is in the C3HeB/FeJ background. Wild-type little males were crossed with *lit/lit* females, and the heterozygous offspring (F1) were interbred to create +/+, *lit*/+, and *lit/lit* genotypes. C3H shiverer mice were also interbred to produce C3H mice for study. The hybrid mouse (*lit/lit;shi*/+) was produced by first crossing C57Bl *lit/lit* females with C3H *shi/shi* males to produce a double heterozygote. Male F1 mice were backcrossed to C57Bl *lit/lit* females. Mice were housed in the animal facility at the Clinical Investigations Directorate of Wilford Hall, Lackland Air Force Base, fed standard laboratory chow ad libitum and kept on a 12 h dark/light schedule.

Mutant genotyping: A method was developed to genotype the little locus (Ghrhr) by PCR and

subsequent restriction analysis (17). The shiverer locus (MBP) was determined by Southern analysis as previously published (18). A 581-bp probe that spanned the deletion breakpoint was designed for this purpose.

Evaluation of brain MBP and PLP mRNA and MBP protein: Brains were harvested immediately after death induced by carbon dioxide inhalation. The left hemisphere was frozen in liquid nitrogen and stored at -20°C for protein analysis and the right hemisphere was homogenized in 4M guanidinium thiocyanate buffer for RNA isolation. Total RNA was extracted using a protocol adapted from Chomczynski and Sacchi (19). Five μg of total RNA were electrophoresed through a 1.2% denaturing agarose gel, transferred onto a GeneScreen membrane (DuPont NEN) and UV crosslinked. The membrane was hybridized with a radiolabeled cDNA probe for the 14kD form of mouse MBP (gift of Dr. Carol Readhead, Cedar Sinai School of Medicine) according to Church and Gilbert (20). The membrane was exposed for 24 hr to a phosphorimager screen and quantitation was done by ImageQuant version 3.2 (Molecular Dynamics, CA). The membrane was subsequently stripped in 50mM sodium phosphate in 55% formamide at 65°C for 60 min. and rehybridized with a radiolabeled cDNA probe for mouse cyclophilin (Ambion, Inc., Austin TX). Following quantitation and stripping, the membrane was hybridized with a radiolabeled cDNA probe, BAS1013, for mouse PLP (gift of Dr. Anthony Campagnoni, UCLA). Since it has been reported (21) that cyclophilin mRNA levels slightly decrease over the first 40 days of postnatal life, the membranes were also rehybridized with a cDNA probe for α-tubulin (21). The message levels for MBP and PLP were normalized to the cyclophilin mRNA abundance or to the α-tubulin mRNA abundance. Since the relative values were the same, only the message levels normalized to cyclophilin abundance are reported.

MBP protein analysis was done using a radioimmunoassay kit purchased from Diagnostic Systems Laboratories (Webster TX). The frozen left hemisphere of each brain was thawed on ice and immediately homogenized in 5 ml cold sterile H_20. The homogenate was centrifuged at 3000g for 20 min at 4°C. The supernatant was diluted in 0.2M Tris-acetate buffer, pH 7.2, containing 1% Triton X-100 and 0.1% aprotinin (22), and an aliquot was used to measure MBP concentration. MBP concentration was normalized to total protein concentration as measured by the Bio-Rad DC colorimetric assay (Richmond CA).

IGF-1, GH and TSH quantitation: Blood was collected from mice by cardiac puncture. Serum was separated from the cellular components and frozen. Fifty µl of serum was used per assay; assays were performed in duplicate. Each sample was acid-extracted using C-18 cartridges (Sep-Pak, Waters Associates) and IGF-1 assayed by radioimmunoassay. Serum assay of IGF-1 was performed by Dr. Ross Clark at Genentech, Inc., San Francisco, CA. Anterior pituitaries were harvested for analysis of intrapituitary GH and TSH, weighed, homogenized in 500 µl 0.05M PBS with 1% BSA, and stored at -20°C. At the time of assay, the homogenate was centrifuged at 8,000g for 20 min at 4°C. The supernatant was used for analysis with enzyme immunosorbent assay (EIA) kits purchased from Amersham (Arlington Heights, IL) for either rat GH or TSH.

Histological analysis of CNS myelin: 60-day old mice were euthanized by isoflurane inhalation, and brain and spinal cord were removed and fixed in 10% buffered formalin for 1-3 days. The brains were then bisected and placed into histology cassettes. The spinal cord tissue was bisected to show a cross section and sectioned lengthwise depending on the size of the tissue. The tissues were processed in a Shandon Lipshaw processor according to standard techniques (Carson, 1997). They were than embedded in paraffin and sectioned. Semithin sections of 8µm of the brains were cut sagittally, and the spinal cord was sliced at 4µm. The sections were then deparaffinized and hydrated to 95% ethanol and placed in 0.1% luxol fast blue solution overnight at 55°C. The slides were rinsed in 95% ethanol followed by distilled water and then dipped in lithium carbonate and differentiated in 70% ethanol. They were counterstained with cresyl echt violet. Size measurements of white matter regions were made with the assistance of ImagePro (Media Cybernetics, Silver Springs, MD).

Electron microscopy of optic nerves and brain: 60-day mice and controls (n=5 for each) were deeply anesthetized with sodium pentobarbital (100 mg/kg), and transcardically perfused with 1% paraformaldehyde and 2.5% glutaraldehyde in 0.1M phosphate buffer, ph 7.4, at 25°C. The brain and the optic nerve connected to the eye were removed and fixed overnight in the same fixative at 4°C. The brain was sagittally sliced in ~0.5 mm of thickness in the region containing the anterior commissure and the corpus callosum. The tissues were then washed in 0.1M phosphate buffer, postfixed in 1% OsO_4 in the same buffer, rinsed with H_20, dehydrated through a graded series of

ethanol and propylene oxide, and directionally embedded in epoxy resin (Polybed 812, Polysciences, Inc, Warrington, PA). Semithin sections of ~1μm of the optic nerves were cut perpendicular to the longitudinal axis of the nerves at a point 1 mm behind the retina. Sections were stained with 7% aqueous uranyl acetate and counterstained with Reynolds' lead citrate (Hayat, 1970) using a microwave staining procedure (25). Semithin sections of the brain tissue containing the anterior commissure were cut sagittally and processed in the same manner. The sections were examined with a Philips 301 transmission electron microscope (Philips Electronic Instruments Co, Mahwah, NJ, USA).

Six to eight photographs were randomly taken from each anterior and posterior part of the anterior commissure and from each corpus callosum at 10,000X. Each negative was printed to give a final 30,000X magnification. The axon size and thickness of myelin sheaths were measured with the aid of the Image-Pro analysis system. Only those axons that were perpendicular to their long axis and in which both the inner and outer surface of the myelin sheath was sharp and distinct were used in this analysis. The diameter of axons was calculated from the circumference of the inner surface of the myelin sheaths. The thickness of myelin sheaths was measured by determining the circumference of the outer surface of the sheath and using the approximation as calculated by ImagePro which subtracts the axon circumference and corrects for the shape of the image.

Visual Evoked Potentials: Flash visual evoked potentials (FVEPs) were recorded from the mutant and wild-type control (n=11 for each) mice. The mice were anesthetized with ketamine and xylazine (75 mg/kg and 10mg/kg, respectively for wild-type and little mice, and 60 mg/kg and 8 mg/kg, respectively for shiverers) under normal room illumination. They were placed prone on a sling, and normal body temperature was maintained by use of a surrounding hot water bag. The mice were placed facing the flash lamp diffusing face plate (Grass PS 22 Photostimulator) at a distance of 20 cm. Corneas were kept moist with saline or 2.5% hydroxypropyl methylcellulose (Goniosol, Johnson & Johnson). Stainless steel needle electrodes were placed subdermally in the occipital midline (active) and the ear (reference). The active electrode was shortened to 6 mm length and re-sharpened and then inserted posteriorly so that its tip was not anterior to the interaural line in an attempt to reduce interference by the electroretinogram (ERG). A subdermal needle electrode in the midline near the tail served as the ground electrode. The signals were amplified by 10,000 and filtered

from 1-1000Hz (Grass P5 amplifier). The amplified signals containing both electroencephalographic and electrocardiographic activity were monitored on the screen of an oscilloscope (Tektronix 5110). The amplified signals were also digitized and recorded by a Nicolet 4094 digital oscilloscope set for averaging (0.396 s trace, digitization rate = 10,000/s). During recording of FVEPs, ambient illuminance was dim (2.9 lx) as measured at the eye with a light meter (International Light IL 1700 radiometer with illuminance detector). The surrounding luminance was 0.3 to 0.6 fL (Minolta 1 degree Spotmeter). The mice were stimulated binocularly at 1 flash/s. Flash intensity was set at 16, which produced 88 lx s (Gossen Luna Pro light meter) illumination at the eyes. One hundred twenty traces synchronized with flash onset were averaged. Four FVEPs were recorded from each mouse. Noise controls were produced in the same way but with the flash occluded by a black opaque cloth. The digitized waveforms were saved as ASCII files using a commercial software analysis package (Vu-Point). The average of the four FVEPs was computed and used as the measured datum for each mouse.

RESULTS

Myelin characterization of little mice:

MBP and PLP levels in brain from little mice

Although there is extensive data on the effect of GH/IGF-1 on myelination, there is no information on the specific effect of GH/IGF-1 on MBP *in vivo*. The period of maximal MBP expression in mice is between 10 and 30 days after birth with the peak at about 15 days (26). Thereafter, expression declines and plateaus at a much lower level. Therefore, MBP expression was determined at 18, 25 and 60 days postnatal in little mice. As seen in figure 2, MBP mRNA expression in little mice is lower than wild-type mice, but is only significant at 60-days. However, there is no difference in MBP protein levels between little and wild-type mice at any age tested. Therefore, any hypomyelination of little mice cannot be attributed to insufficient MBP expression.

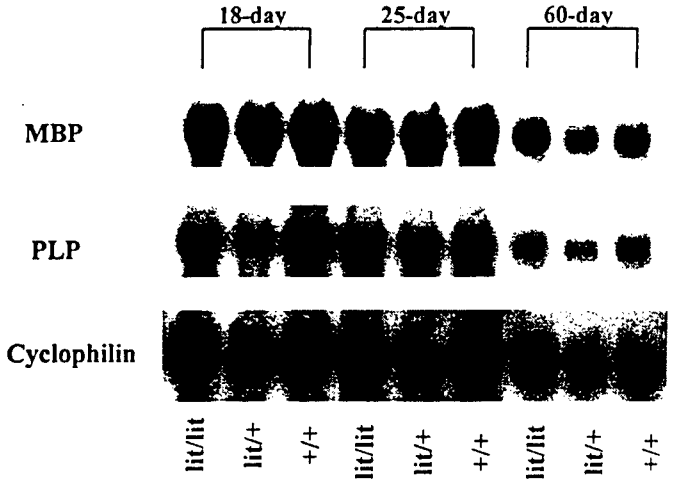

Figure 1. Northern analysis of MBP and PLP mRNA in little mice.

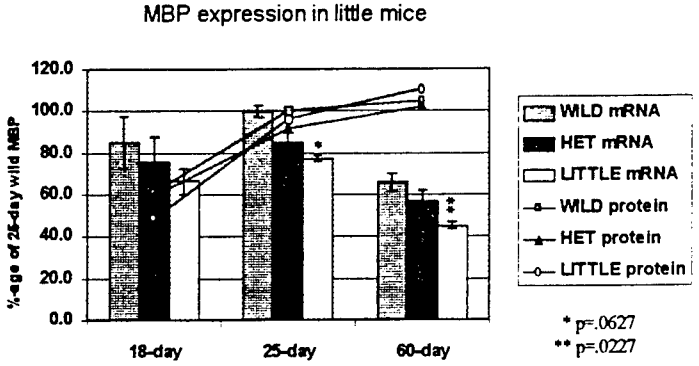

Figure 2. Quantitation of MBP mRNA and protein in little mice. MBP mRNA data are shown as a ratio of MBP mRNA to cyclophilin mRNA.

Since MBP protein levels were found to be normal in little mice, expression levels of PLP were also determined. Figure 3 shows that PLP mRNA levels in little mice were no different from wild-type; therefore, protein levels were not measured. These results indicate that low PLP is not responsible

for any hypomyelination in the little mice.

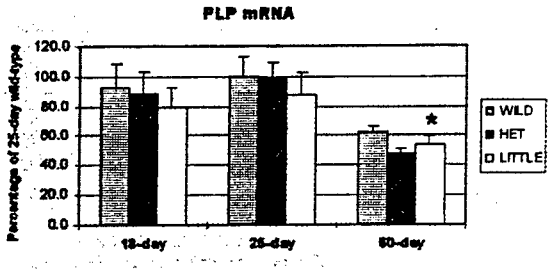

* p = .0677

Figure 3. Quantitation of PLP mRNA in little mice. Data are shown as a ratio of PLP mRNA to cyclophilin mRNA.

Morphometric analysis of white matter tracts and optic nerve in little mice

Our molecular analyses of myelin proteins are inconsistent with the literature reporting hypomyelination in the little mice; therefore, a morphometric analysis of the major CNS myelinated regions was done in order to confirm or refute these reports. The thickness of myelin sheaths, axon sizes, and density of myelinated axons were measured in the corpus callosum, anterior commissure, and the optic nerve in little and wild-type mice. The corpus callosum and anterior commissure were selected for study because these regions have previously been shown to be abnormally myelinated in IGF-1 knockout and IGFBP-1 mice (8,9). As shown in tables 1 and 2, our results indicate no difference in either the thickness of myelin sheaths or the density of myelinated axons in the corpus callosum. Since myelin thickness increases with increasing axon diameter, the myelin sheaths of comparable axon sizes were compared. Additionally, no difference in average axon diameter in these white matter regions was seen. The results for the anterior commissure are shown in tables 1 and 3. The density of the myelinated axons is similar between little mice and wild controls in both the anterior and the posterior region. Moreover, the thickness of the myelin sheaths in both regions is not reduced in the little mice. In contrast, our data indicates a statistically significant increase in average myelin thickness of axons less than 1000 nm in diameter within the posterior region of the anterior commissure of the little mouse as compared to the wild-type controls.

Table 1. The density of myelinated axons in little and wild-type mice

	Corpus callosum	Anterior commissure (anterior)	Anterior commissure (posterior)
Little	38.2 ± 9.3	64.4 ± 26.6	38.3 ± 11.7
Wild	41.9 ± 12.5	69.8 ± 14.9	46.4 ± 20.3

The number of myelinated axons was counted on each electron microphotograph. Values are means ± SD.

Table 2. Myelin sheath thickness in corpus callosum

		< 500 nm	500-800 nm	> 800 nm
Little	Avg. myelin thickness (Median)	94.9 ± 15.3 (93.9)	105.6 ± 25.0 (101.1)	131.3 ± 41.7 (119.4)
	Avg. axon diameter	399.8 ± 71.2 [23.4%]	637.6 ± 88.0 [45.4%]	1093.1 ± 307.1 [31.2%]
Wild	Avg.myelin thickness (Median)	92.7 ± 15.4 (90.7)	108.8 ± 72.6 (102.0)	131.4 ± 32.0 (126.8)
	Avg. axon diameter	414.2 ± 71.6 [24.0%]	641.2 ± 82.0 [49.0%]	1027.5 ± 233.8 [27.0%]

Values are means ± SD. The percentage of axons analyzed is shown in brackets.

Table 3. Myelin sheath thickness in anterior commissure

Anterior	region	< 500 nm	500-700 nm	> 700 nm
Little	Avg. myelin thickness (Median)	95.2 ± 27.9 (90.3)	105.9 ± 25.2 (103.4)	128.6 ± 34.6 (125.8)
	Avg. axon diameter	410.8 ± 75.2 [20.4%]	597.7 ± 57.7 [36.1%]	974.4 ± 274.6 ** [43.5%]
Wild	Avg.myelin thickness (Median)	93.7 ± 21.6 (89.5)	101.6 ± 27.3 (98.1)	124.2 ± 29.4 (120.4)
	Avg. axon diameter	396.2 ± 69.5 [40.2%]	584.8 ± 58.5 [36.6%]	884.4 ± 169.6 [23.2%]

Posterior	region	< 700 nm	700-1000 nm	> 1000 nm
Little	Avg. myelin thickness (Median)	107.3 ± 20.5 * (106.4)	124.2 ± 25.1 * (118.9)	144.0 ± 31.3 (144.7)
	Avg. axon diameter	552.3 ± 106.8 [25.2%]	857.1 ± 79.7 [31.1%]	1318.9 ± 273.3 [43.7%]
Wild	Avg.myelin thickness (Median)	85.2 ± 19.7 (84.0)	107.2 ± 23.9 (103.2)	134.2 ± 37.0 (126.2)
	Avg. axon diameter	543.2 ± 124.9 [37.7%]	845.0 ± 86.3 [39.4%]	1228.8 ± 210.7 [22.8%]

Values are means ± SD. The percentage of axons analyzed is shown in brackets. * $p<0.05$; ** $p<0.01$ versus controls.

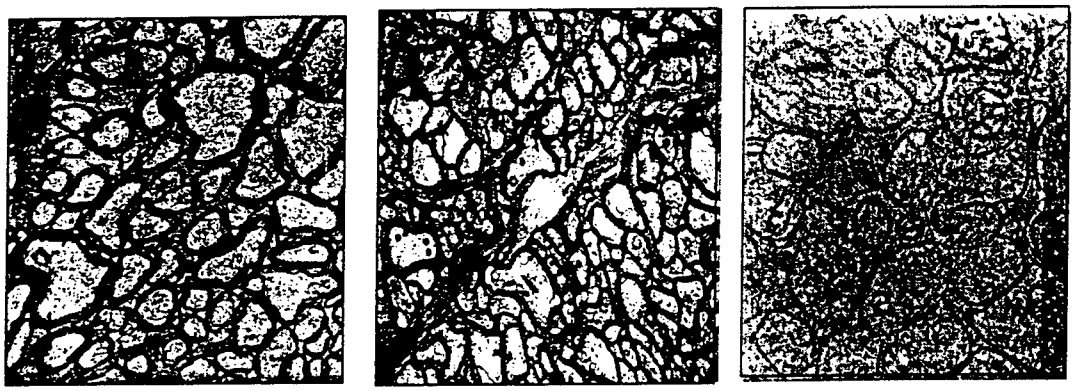

+/+ x7,800 shi/+ x 7,100 shi/shi x 18,000

Figure 4. Electronmicrographs of the optic nerves in little, wild, and shiverer mice. The shiverer mouse is shown for comparison to a known hypomyelinated mouse.

Size of white matter tracts

Our morphometric analyses suggest that the little mice have CNS myelination of comparable thickness and density to the wild-type mouse. This conflicts with previously reported data showing retarded neuronal growth, an underdevelopment of axons and dendrites, of layer 5 of area 6 of Caviness in the motor cortex (12). However, since the little mouse brain is known to be smaller than the wild brain, it is possible that the corpus callosum and anterior commissure are smaller as well. In order to reconcile this discrepancy, the sizes of these regions were compared by histological

methods. Comparable serial sections were compared in the little and control mice and the area of each region was calculated. One of these sections in shown in figure 5. The area of the anterior commissure of the little mouse is calculated to be 75.9% that of the wild mouse, and the area of the corpus callosum is 82.1% that of the wild mouse.

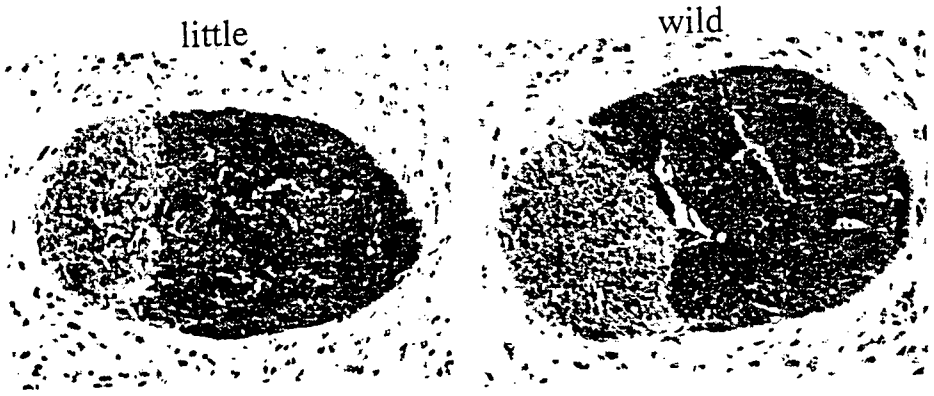

Figure 5. Relative size of the anterior commissure in little mice and wild controls.

Visual evoked potential testing of little mice

Although the morphology and quantity of myelin appears normal in little mice, the function had not been determined. We selected a noninvasive FVEP test procedure in order to correlate this study with the human studies of 18q- syndrome. The averaged plots of the little mice and wild controls are shown in figure 6. The first positive peak represents the eye response (the electroretinogram) which was difficult to avoid recording since the size of the mouse's heads was so small. The implicit time to first negative peak and also to the first positive peak of the cortical response are very reproducible. There is no significant difference between the waveforms of the little and control mice. We had initially tested a group of shiverer mice and their wild-type littermates to establish the feasibility of distinguishing hypomyelinated animals using this procedure. The first major negative and positive peaks were significantly delayed in the shiverer mutants (data not shown).

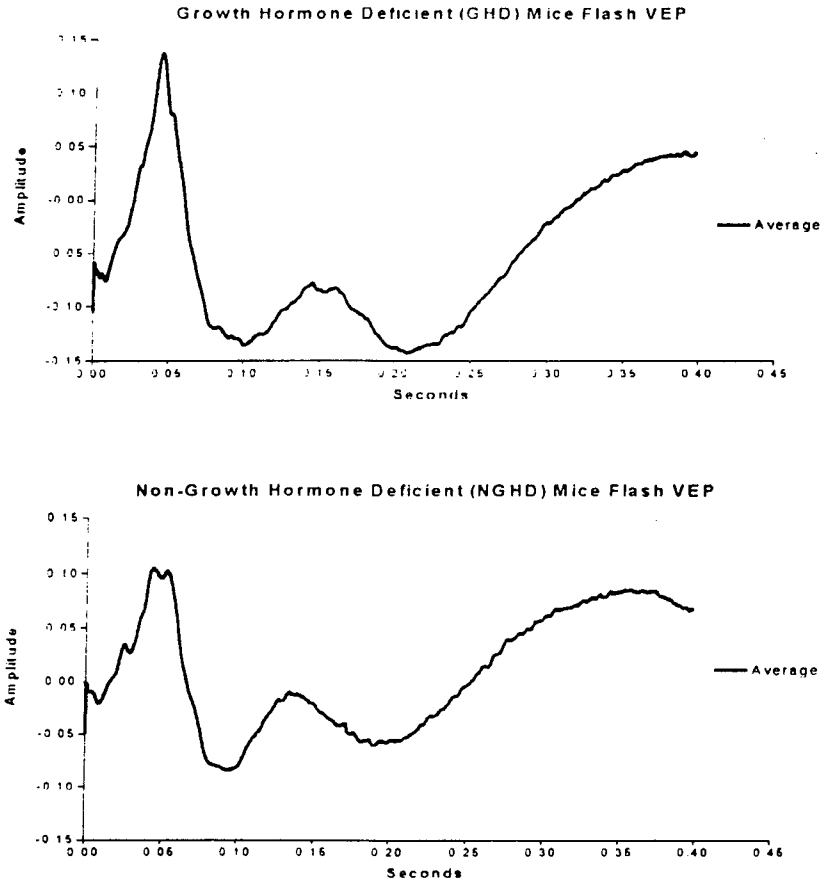

Figure 6. FEVPs for little (growth hormone deficient) and wild mice.

Endocrine characterization of shiverer mice:

Serum IGF-1 and intrapituitary GH levels in shiverer mice

No information is available on the impact of the shiverer mutation on the neuroendocrine axis. Because of interest in the potential effect of an abnormality of MBP on GH production, serum IGF-1 of 42-day old shiverer and control mice was assayed (Figure 7). Due to the pulsatile nature of GH secretion, random serum GH determination does not provide useful information; therefore, IGF-1 was chosen as an initial marker for GH production. Since the number of 42-day old control animals is small, statistical evaluation could not be undertaken; however, a trend is apparent. Assays on additional animals may make these data significant. The functional significance of these changes on parameters other than somatic growth has not been evaluated. The results encouraged us to measure intrapituitary GH levels, so pituitaries were harvested from 60-day mice and assayed (Figure 7).

These data indicate no significant difference in pituitary GH production and release between the little mice and normal controls.

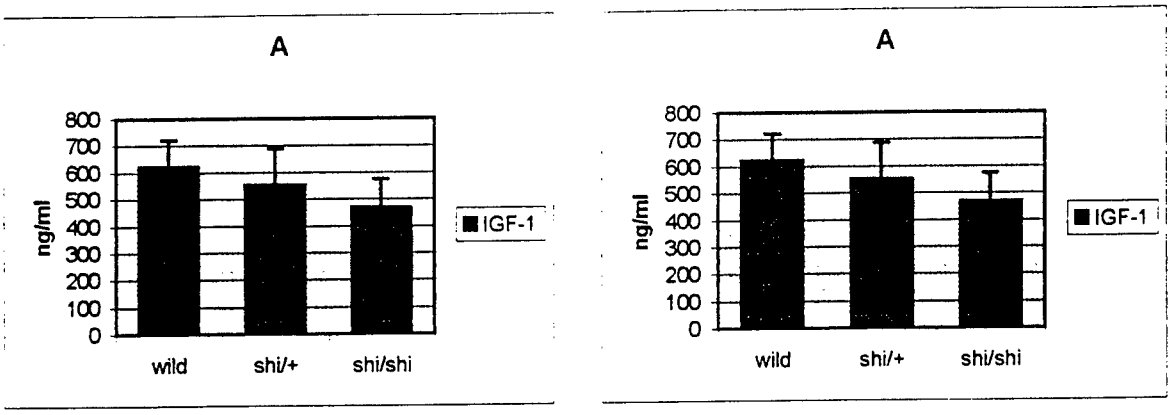

Figure 7. Serum IGF-1 levels (A) and intrapituitary GH levels (B) in little and control mice. Values are means ± SD.

Hybrid mouse model:

Development of hybrid mouse model

We have demonstrated that the hybrid (*lit/lit; + shi*) is viable. EM analysis is being conducted to establish the level of myelination in these hybrids and to determine if this differs from the *+ +; + shi* and the *lit/lit; + +* mice during development. Unfortunately, the level of MBP expression could not be evaluated in these hybrids as proposed due their strain differences. These mice are crosses of the C57Bl and C3H strain. During the course of these studies, we discovered that the C3H strain produces almost twice as much MBP as the C57Bl strain; therefore, crossing them results in a large amount of individual variability in MBP expression.

MBP expression following GH treatment:

Because of the unexpected complications with measuring MBP expression in the hybrid mouse, we altered our experimental plan. To answer the question of whether GH treatment enhances MBP expression in an animal that expresses less than normal amounts, we treated shi/+ animals that express only 50% of normal levels of MBP. To date, two groups of 7 shiverer heterozygote mice have

received daily GH injections for 30 days commencing on postnatal day 5. Three groups of approximately 7 shi/+ mice have received saline injections for the same interval. The mice were weighed every 5 days throughout the treatment phase and then sacrificed at the age of 65 days. Brains were weighed and harvested for RNA and protein analysis. These analyses are being initiated. Additionally, one mouse from each group was perfused and the brain isolated for electron microscopic analysis as described for the little mouse above.

DISCUSSION

GH-deficient little mice have previously been reported to be hypomyelinated (10), and this led us to propose the development of a hybrid mouse model that is heterozygous for MBP in a growth hormone deficient background. We hypothesized that there may be synergistic effects between the two conditions that could result in even less myelin production. To examine this, we began by establishing the level of MBP expression and myelination in the presumed hypomyelinated little mouse for comparison to the hybrid. We discovered that the levels of two major myelin proteins, MBP and PLP, were essentially normal in these mutants during the course of development. Moreover, morphometric analysis of myelin sheaths in brain major white matter tracts showed no difference in myelinated axon density, size, and myelin sheath thickness between little mutants and their wild controls. Histological analysis indicated that the size of these white matter tracts is reduced proportional to the reduction in brain size of the little mouse as compared to the wild controls. In summary, the little mouse appears to have a smaller brain and proportionately smaller white matter regions that are otherwise normal with regard to myelination.

The myelin appears normal in structure and quantity in little mice, but the function remained in question. Since auditory evoked brainstem responses have been used as a functional measure of myelination in shiverer mutants (27) as well as humans, we initially attempted this test with little mice. Unfortunately, we discovered that ABRs of little mutants are abnormal in that signal processing beyond the cochlea is disrupted. This could be due to structural abnormalities of the ear as a result of GH deficiency. Therefore, FVEPs were conducted on the little mice as a means of measuring CNS function. Our results show no functional difference as measured by the FVEP between little mice and controls. This further supports our conclusion of normal CNS myelin in the little mouse. These

results were quite unexpected and provide interesting information regarding the impact of naturally occurring growth hormone deficiency on myelination. A publication reporting these results is in progress.

This study also generated valuable results when further characterizing the shiverer mouse. 18q- patients are haploinsufficient for MBP, but their cause of GH-insufficiency is unknown. The GH-insufficiency region on chromosome 18 has been narrowed (14), and the MBP gene lies within this region. To determine whether MBP could be a candidate gene for GH-deficiency/insufficiency in 18q- syndrome, we measured serum IGF-1 and intrapituitary GH levels in shiverer mutant mice and controls. The IGF-1 data indicate that homozygous shiverer mice have reduced circulating levels of this factor at 42 days. Since the number of control animals is small, statistical significance could not be determined. In contrast, pituitary GH levels in shiverer mice appear to be normal. Thus, this data likely rules out MBP as a candidate gene for GH-deficiency in 18q- syndrome.

Development of a hybrid mouse model that has only one copy of the MBP gene in a GH-deficient background we hoped would prove useful in examining the relationship between GH and MBP production *in vivo*. We have shown that this hybrid is viable and are conducting limited studies to determine the consequences of GH-deficiency on MBP haploinsufficiency.

Treatment of heterozygous shiverer mice with pharmacological doses of GH during early postnatal development may elucidate whether intervention with GH enhances MBP production. It has been shown that GH has a positive effect on myelination, but the specific effect on MBP expression is not known. Two groups of shi/+ mice have completed GH treatment and their brains have been collected for analysis. Also, tissues from two groups of saline-treated shi/+ controls have been harvested. The analyses are in progress.

REFERENCES

1. Barbarese, E. et al. The effect of the shiverer mutation on myelin basic protein expression in homozygous and heterozygous mouse brain. J. Neurochem. 40(6): 1680-1686, 1983.

2. Roth, H.J. et al. Expression of myelin basic protein genes in several dysmyelinating mouse mutants during early postnatal brain development. J. Neurochem. 45(2): 572-580, 1985.

3. Readhead, C. et al. Expression of a myelin basic protein gene in transgenic shiverer mice: correction of the dysmyelinating phenotype. Cell 48: 709-712, 1987.

4. Popko, B. et al. Myelin deficient mice: expression of myelin basic protein and generation of mice with varying levels of myelin. Cell 48: 713-721, 1987.

5. Almazan, G. et al. Epidermal growth factor and bovine growth hormone stimulate differentitaion and myelination of brain cell aggregates in culture. Develop. Brain Res. 21: 257-264, 1985.

6. D'Ercole, AJ. Et al. Brain growth retardation due to the expression of human insulin like growth factor binding protein-1 in transgenic mice: an in vivo model for the analysis of igf function in the brain. Develop Brain Res. 82:213-222, 1994.

7. Ye, P. et al. In vivo actions of insulin-like growth factor-1 (IGF-1) on brain myelination: studies of IGF-1 and IGF binding protein-1 (IGFBP-1) transgenic mice. J Neurosci. 15(11): 7344-7356, 1995.

8. Mozell, R.L. et al. Insulin-like growth factor I stimulates oligodendrocyte development and myelination in rat brain aggregate cultures. J. Neurosci. Res. 30: 382-390, 1991.

9. Beck, K.D. et al. Igf1 gene disruption results in reduced brain size, CNS hypomyelination, and loss of hippocampal granule and striatal parvalbumin-containing neurons. Neuron 14: 717-730, 1995.

10. Carson, M.J. et al. Insulin-like growth factor I increases brain growth and central nervous system myelination in transgenic mice. Neuron 10: 729-740, 1993.

11. Godfrey, P. et al. GHRH receptor of little mice contains a missense mutation in the extracellular domain that disrupts receptor function. Nature Genet. 4: 227-232, 1993.

12. Noguchi, T. Effects of growth hormone on cerebral development: morphological studies. Hormone Res. 45: 5-17, 1996.

13. Ghidoni, D.P. et al. Growth hormone deficiency associated with the 18q- syndrome. Amer. J. Med. Genet. 69: 7-12, 1997.

14. Cody, J.D. et al. Growth hormone insufficiency associated with haploinsufficiency at 18q23. Amer. J. Med. Genet. 71: 420-425, 1997.

15. Hale, D.E. Growth failure and growth hormone deficiency in 18q- syndrome. Pediatr. Res. 37: 90A, 1995.

16. Gay, C.T. Magnetic resonance imaging demonstrates incomplete myelination in the 18q- syndrome. Evidence for myelin basic protein haploinsufficiency. Neuropsyc. Genet. 74: 422-431, 1997.

17. Lehman, D.M. et al. Rapid typing of the little mouse mutation. Mouse Genome 95(3): 689-691, 1997.

18. Molineaux, S.M. et al. Recombination within the myelin basic protein gene created the dysmyelinating shiverer mouse mutation. PNAS 83: 7542-7546, 1986.

19. Chomcynshi, P. and Sacchi, N. Single-step method of RNA isolation by acid guanidinium thiocyanate-pheno-chloroform extraction. Analyt. Biochem. 162: 156-159, 1987.

20. Church, G.M. and Gilbert, W. Genomic Sequencing. Proc Natl Acad Sci USA 81: 1991-1995, 1984.

21. Cowan, N.J., et al. Expression of human alpha-tubulin genes: interspecies conservation of 3' untranslated regions. Mol Cell Bio. 3: 1738-1745, 1983.

22. Shine, H.D. et al. Morphometric analysis of normal, mutant, and transgenic CNS: correlation of myelin basic protein expression to myelinogenesis. J Neurochem 58(1): 342-349, 1992

23. Carson, F.L. Histotechnology. A self-instructional text. 2nd ed. American Society of Clinical Pathologists. pp 96-97, 1997

24. Hayat, M.A. et al. Staining. In: Principles and Techniques of Electron Microscopy, Biological Applications 1, pp 262-264 and 345, Van Nostrand Reinhold Co, New York, 1970

25. Estrada, J.C. et al. A rapid method of staining ultrathin sections for surgical pathology TEM with the use of the microwave oven. Am J Clin Path 83: 639-641,1985

26. Carson, J.H. et al. Developmental regulation of myelin basic protein expression in mouse brain. Develop. Biol. 96: 485-492, 1983.

27. Fujiyoshi, T. et al. Restoration of brain stem auditory-evoked potentials by gene transfer in shiverer mice. Ann. Otol. Rhinol. Laryngol. 103: 449-456, 1994.